Tectonic feedback, intraplate orogeny and the geochemical structure of the crust: a central Australian perspective

M. SANDIFORD[1], M. HAND[2] & S. McLAREN[2]

[1] *School of Earth Sciences, University of Melbourne, Victoria, Australia (e-mail: m.sandiford@earthsci.unimelb.edu.au)*

[2] *Department of Geology and Geophysics, University of Adelaide, South Australia*

Abstract: The geological record of intraplate deformation in central Australia implies that past tectonic activity (basin formation, deformation and erosion) has modulated the response of the lithosphere during subsequent tectonic activity. In particular, there is a correspondence between the localization of deformation during intraplate orogeny and the presence of thick sedimentary successions in the preserved remnants of a formerly widespread intracratonic basin. This behaviour can be understood as a kind of 'tectonic feedback', effected by the long-term thermal and mechanical consequences of changes in the distribution of heat producing elements induced by earlier tectonism. From a geochemical point of view, one of the most dramatic effects of intraplate orogeny in central Australia has been the exposure, in the cores of the orogens, of deep crustal rocks largely depleted in the heat producing elements. The geochemical structuring of the crust associated with the erosion of the heat-producing upper crust resulted in long-term cooling of the deep crust and upper mantle with associated lithospheric strengthening. This is illustrated here by mapping the consequences of deformation and associated tectonic responses onto the h–q_c plane, where h is the characteristic length-scale for heat production distribution, and q_c is the total crustal heat production. Because rates of intraplate deformation in central Australia appear to be much slower than that typical of plate margin orogens, it is possible that the ongoing geochemical structuring of the crust has played an important role in terminating intraplate orogeny in central Australia by providing a 'thermal lock'. The diagnostic geophysical signature of this lock may be the extraordinary gravity anomalies of the central Australian intraplate orogens.

Central Australia provides an intriguing record of intraplate deformation resulting in the development of a number of extraordinary orogens that expose deep crustal rocks in their cores (Forman 1971; Teyssier 1985; Goleby *et al*. 1989). The spatial distribution of intraplate deformation during the Alice Springs and Petermann orogenies suggests that the mechanical response of this region has varied through time. Consequently, this response is important for our understanding of the processes controlling reactivation in intraplate settings. In previous contributions it has been argued that the distribution of deformation in central Australia has been strongly influenced by prior tectonic processes, such as basin formation and erosion (Sandiford & Hand 1998*a*; Hand & Sandiford 1999). This paper focusses on the way in which intraplate deformation modifies the geochemical structure of the crust in this region, in particular the distribution of heat sources. Recognizing that the distribution of heat sources provides a first-order control on the thermal structure of the crust, the consequences of intraplate deformation for the long-term thermal and mechanical evolution of the crust is then explored. Our aim is to demonstrate the relevance of a novel style of 'tectonic feedback' which seems to have modulated the long-term tectonic behaviour of the central Australian region, and which may be relevant to continental interiors in general. The notion of tectonic feedback is compatible with a highly temperature dependent lithospheric rheology, as suggested by many experimental studies of natural rocks. Such feedback has profound implications for the long-term tectonic evolution of continental interiors, particularly their potential for reactivation.

The record of intraplate deformation in central Australia

Central Australia encompasses the region comprising northern South Australia, the central and southern parts of the Northern Territory, and the

From: MILLER, J. A., HOLDSWORTH, R. E., BUICK, I. S. & HAND, M. (eds) *Continental Reactivation and Reworking*. Geological Society, London, Special Publications, **184**, 195–218. 1-86239-080-0/01/$15.00

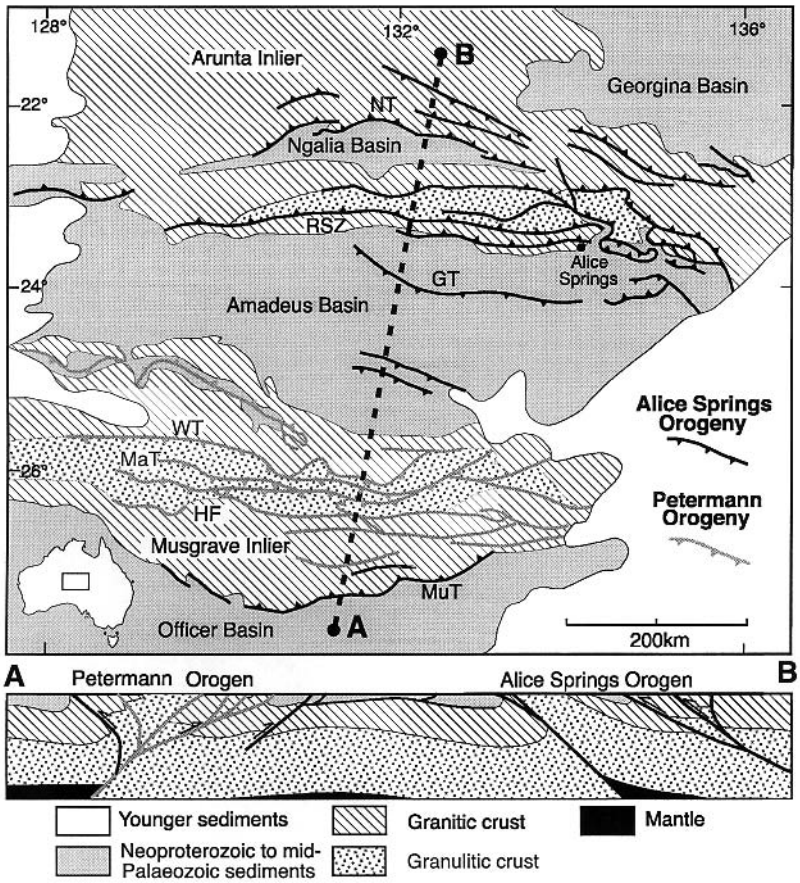

Fig. 1. Geological map and crustal scale-cross section of the central Australian region, showing the structurally remnant Neoproterozoic basins (the Officer, Amadeus, Ngalia and Georgina Basins), separated by basement inliers (the Musgrave and Arunta Inliers). Within the inliers we can distinguish two distinct types of terrane: (1) gneissic granite terranes that form the peripheral regions of the inliers and which are unconformable overlain by the Neoproterozoic sediments; (2) mafic granulite terranes that define the cores of the inliers and which are tectonically juxtaposed with the gneissic granite terranes. This juxtaposition reflects, in part, the strain associated with intraplate orogeny accumulated during the exhumation of the basement inliers from beneath a formerly more or less continuous intracratonic basin. Crustal scale cross-sections based on seismic reflection profiling (Goleby *et al.* 1988, 1989) show that the mafic granulite terranes are representative of the Central Australian lower crust, while the gneissic granite terranes are representative of the mid-upper crust. The central Australian intraplate orogens are characterised by extraordinary gravity anomalies (Mathur 1976). These gravity anomalies are amongst the largest known from the continental interiors. Moreover, they clearly relate to structures that were active during the Petermann and Alice Springs Orogenies. GT, Gardiner Thrust; HF, Hinckley Fault; NT, Napperby Thrust; RSZ, Redbank Shear Zone; UT, Uluru Thrust; WT, Woodroofe Thrust.

contiguous parts of Western Australia (Fig. 1). During the Neoproterozoic this region was largely covered by an extensive intracratonic basin. The record of intraplate deformation in this region is preserved in structures associated with the formation of this basin as well as its subsequent structural dismemberment. This record has been well documented in numerous publications by the Australian Government Survey Organization (AGSO) and its predecessor, the Bureau of Mineral Resources (BMR). In this section, a brief synopsis of this record as largely elucidated by AGSO and BMR geologists is provided, concentrating on the evolution of intraplate orogeny.

Central Australia comprises Palaeo- to Mesoproterozoic, intermediate – high grade, metamorphic complexes overlain by an extensive

system of Neoproterozoic to Phanerozoic basins (Fig. 1). The main crust forming events occurred in the intervals 1900–1600 Ma and 1100–1000 Ma, by which time the region was apparently largely cratonized. From about 800 Ma, regional scale subsidence resulted in widespread sedimentation as reflected in the sequences preserved in the Officer, Amadeus, Ngalia, Georgina and Wiso Basins. These basins are now separated by inliers of older metamorphic 'basement'. The general absence of facies changes and thickness variations in the sediments adjacent to these boundaries, and the continuity of stratigraphy between basins (e.g. Walter *et al.* 1995), provides a compelling argument for the former continuity of these basins. The formerly more or less continuous basin that is assumed to have covered almost the entire Central Australian region through the Neoproterozoic, prior to its fragmentation into the present series of structural-remnant basins, has been termed the Centralian Superbasin.

The fragmentation of the Centralian Superbasin began in the latest Neoproterozoic with the exhumation of the Musgrave Inlier in northern South Australia, which effectively isolated the Officer Basin from the rest of the Centralian Superbasin (Fig. 1). This period of exhumation accompanied the Petermann Orogeny (570–530 Ma), the first of two major intraplate orogenies to have affected the central Australian region. The second major episode, in the Devonian and Carboniferous (430–300 Ma), is known as the Alice Springs Orogeny.

The Petermann Orogen forms an east–west trending belt, with the principal locus of deformation centred on the northern part of the Musgrave Inlier in the vicinity of the Woodroffe and Mann Faults. Along the northern margin of the orogen, differential denudation across large-scale thrust faults resulted in important structuring of the crust. The major structural feature is the Woodroffe Thrust; a south-dipping mylonite zone up to 3 km thick (Edgoose *et al.* 1993; Camacho *et al.* 1995; Stewart 1995) offsetting the Moho by *c.* 20 km (Lambeck & Burgess 1992) and associated with a prominent gradient in the gravity field. South of the Woodroffe Thrust, deformation produced an imbricate thrust stack in which levels of denudation decrease northward from *c.* 40 km to 30 km in the immediate hanging wall of the Woodroffe Thrust (Scrimgeour & Close 1998). The high-pressure rocks are predominantly composed of felsic and mafic orthogneiss. North of the Woodroffe Thrust, mid-crustal rocks are dominated by porphyritic granites and granite gneisses which have been imbricated in a large-scale duplex system that accommodated around 100 km of shortening (Flöttmann & Hand 1999). The structurally higher parts of the duplex contain basal units of the Amadeus Basin, metamorphosed at greenschist to mid-amphibolite facies conditions. Further north within the Amadeus Basin, Petermann-aged structures are defined by submetamorphic, open to tight folding of the Neoproterozoic sequences. The northern margin of the Petermann Orogen thus exposes a near crustal scale cross-section.

As yet there are no definitive estimates for the duration of, or the amount of shortening during, the Petermann Orogeny. Sedimentological and thermochronologic data suggest that the Petermann Orogen began around 570 Ma and continued until about 530 Ma (Maboko *et al.* 1992; Walter & Gorter 1994; Hoskins & Lemon 1995; Walter *et al.* 1995; Lindsay & Leven 1996; Camacho *et al.* 1997). However, in the southern Amadeus Basin sequences older than 570 Ma thicken toward the orogen (Wells *et al.* 1970; Hand & Sandiford 1999), suggesting that loading may have begun prior to 570 Ma, and that the orogeny may have lasted more than 40 Ma. Estimates of shortening along the northern edge of the orogen are constrained by the geometry of Amadeus Basin sequences. However, the bulk of the orogen contains no preserved cover sequences and shortening can only be indirectly inferred from the geometry of, and metamorphic offsets associated with, shear zones. The Woodroffe Thrust dips at around 30° and shows about 12 km of differential offset across it (Scrimgeour & Close 1998), implying that it has accommodated approximately 20 km of shortening. To the south of the Woodroffe Thrust, shear zones typically dip at $\geq 45°$ and the highest pressure rocks are located within a corridor some 30 km wide (Camacho *et al.* 1997). Although by no means definitive, it appears likely that the shortening associated with the Petermann Orogeny was less than <200 km.

The Alice Springs Orogeny resulted in exhumation of the Palaeo to Mesoproterozoic Arunta Inlier from beneath the northern fragment of the Centralian Superbasin isolating the Amadeus and Ngalia Basins from the Georgina and Wiso Basins to the north (Fig. 1). Shortening began possibly as early as 450 Ma (Shaw & Black 1991; Mawby *et al.* 1999), but certainly by 400 Ma, and was marked by the inversion of a late Cambrian to mid-Ordovician marine basin and the deposition of clastic sediment (Shaw *et al.* 1991*a*). Isotopic and sedimentological evidence indicates that deformation continued, at least intermittently, for at least 100 Ma, terminating in the early Permian (Shaw *et al.* 1991*a*; Wells & Moss

1983). Total shortening is estimated at 100–125 km (Teyssier 1985; Flottmann & Hand 1999).

The major Alice Springs structure is the Redbank Shear Zone; a reverse sense shear zone dipping north at *c.* 45° that offsets the Moho by at least 20 km (Goleby *et al.* 1989; Korsch *et al.* 1998). The Redbank Shear Zone is associated with one of the largest gravity anomalies (*c.* 150 mgal) known from continental interiors (Mathur 1976). Early to mid-Devonian syn-orogenic sediments in the northern Amadeus Basin immediately south of the Redbank Shear Zone contain clasts of the underlying sequences including basement (Jones 1972; Jones 1991) indicating that movement on the Redbank Shear Zone was initiated at or before 400–390 Ma (see also Shaw & Black 1991). As with the Woodroffe Thrust in the Petermann Orogen, deformation along the Redbank Shear Zone has produced a crustal-scale lithological subdivision. To the south of the Redbank Shear Zone, the Arunta Inlier exposes large granitic complexes, which have intruded low-pressure amphibolite to greenschist grade metasediments. Immediately north of the Redbank Shear Zone, in the core of the Arunta Inlier, medium pressure mafic and felsic granulite outcrop over a zone up to 50 km across strike.

Further north, in the central part of the Arunta Inlier, the Napperby Thrust carries a basement wedge composed mainly of granite and granite gneisses over sediments in the northern Ngalia Basin (Wells & Moss 1983). The Napperby Thrust was initiated during late Devonian to early Carboniferous (Wells & Moss 1983), at least 50 Ma after deformation began along the Redbank Shear Zone. It accommodated approximately 20 km of shortening on a surface that dips northwards at 30° (Wells & Moss 1983; Bradshaw & Evans 1988). Along the northern margin of the Arunta Inlier, granitic basement has been thrust northward over Neoproterozoic and early Palaeozoic cover sequences belonging to the Georgina and Wiso Basins.

In summary, the Petermann and Alice Springs Orogens show important similarities:

- in both cases, deformation along crustal–penetrative thrust faults has resulted in the formation of major gravity gradients;
- compared with typical plate margin orogens, the total shortening is relatively minor (of the order 100 km); and
- given the limited shortening, the interval over which deformation occurred is relatively long implying slow bulk orogenic shortening rates; in the case of the Petermann Orogeny (where absolute age constraints are relatively poor) the orogen probably lasted at least 40 Ma, while the Alice Springs Orogeny lasted at least 100 Ma and possibly 150 Ma.

Distribution of deformation and sediment thickness in the Centralian superbasin

An intriguing aspect of the record of intraplate deformation in central Australia relates to the way in which the locus of deformation changed in space and time. The Petermann and Alice Springs Orogens appear to be more or less mirror images of each other. Both are characterized by E–W structural trends (reflecting predominant N–S shortening), therefore they must have formed in response to similarly oriented intraplate stress fields. However, it is apposite to ask why the Alice Springs aged deformation was not also localized in the vicinity of the Petermann Orogen but some 300 km further north? This question has been addressed elsewhere in a series of papers (Sandiford & Hand 1998*a*; Hand & Sandiford 1999), which were motivated by the observation that the locus of intraplate deformation appears to mimic the main sedimentary depocentres in the Centralian Superbasin (Fig. 2). In the following section these observations are briefly summarized.

Immediately prior to the Petermann Orogeny, the Centralian Superbasin was thickest (>4 km, Fig. 2a) in the vicinity of the Musgrave Inlier, the region in which deformation was subsequently localized. At the same time a relatively thin sheet (<2 km, Fig. 2a) of sediment covered the Arunta Inlier. Following the Petermann Orogeny the locus of subsidence shifted to the northern part of the Amadeus Basin in the vicinity of the Arunta Inlier, while the major Petermann Orogen structures such as the Woodroffe Thrust were stripped of their cover and exhumed from deep levels (Fig. 2b). Prior to the Alice Springs Orogen, the northern margin of the Amadeus Basin contained at least 6 km of sediment and locally as much as 8 km (Fig. 2b), with isopachs increasing northwards across the basin towards the region where the most intense Alice Springs Orogenic deformation was localized. Importantly, the major Petermann-aged structures such as the Woodroffe Thrust remained inactive during the Alice Springs Orogeny (for more details see Hand & Sandiford 1999).

It is believed that these observations imply that past tectonic activity (basin formation, deformation and erosion) has modulated the response of the central Australian lithosphere during subsequent tectonic activity. This suggests that the link is primarily thermal, with the behaviour

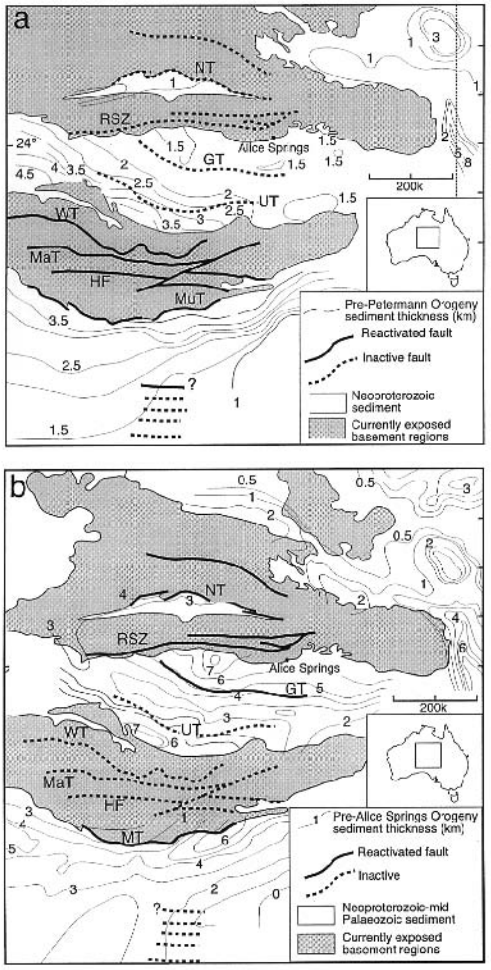

Fig. 2. Isopach maps for the Centralian Superbasin constructed for time intervals immediately prior to the onset of the Petermann Orogeny (Fig. 2a) and the Alice Springs Orogeny (Fig. 2b). Details of these isopach distributions are outlined in Hand & Sandiford (1999). It is noted that prior to the Petermann Orogeny the deepest parts of the basin were in the vicinity of the Petermann Orogen. Following the Petermann Orogeny, which resulted in the exhumation of the Musgrave Inlier, the depocentre shifted north, such that by the time of the Alice Springs Orogen the main sedimentary mass was located in the vicinity of the northern Amadeus basin, and the southern Arunta Inlier, which became the locus of Alice Springs aged deformation. HF, Hinckley Fault; MaT, Mann Thrust; MuT, Munyari Thrust; NT, Napperby Thrust; RSZ, Redbank Shear Zone; UT, Uluru Thrust; WT, Woodroofe Thrust.

reflecting an important example of 'tectonic feedback' effected by the long-term thermal consequences of changes in the distribution of heat producing elements in the crust. In order to quantify the way this feedback has helped to shape the tectonic evolution of this part of the continent, it is necessary to first understand the way in which heat production is distributed in the central Australian crust.

Heat production distributions in the central Australian region

As discussed earlier the Petermann and Alice Springs Orogens show remarkable structural similarities. This similarity extends to the petrological and geochemical character of the orogens. Each is characterized by a high-grade gneissic core granulite comprising significant proportions mafic granulites. This core is tectonically juxtaposed against essentially granitic terranes along the major structures active during the intraplate orogenies. The fact that the sediments of the Centralian Superbasin unconformably overlie these gneissic granite terranes implies that they formed the upper crust prior to basin formation. Seismic reflection and refraction profiling (Goleby *et al*. 1989) together with gravity measurements (Mathur 1976) across the Alice Springs Orogen confirms the fact that the mafic granulites exposed in the core of the orogen connect directly with, and are therefore representative of, the mid-lower crust beneath the basins, while the granitic terranes connect with the mid-upper crust (Fig. 1). By virtue of the fact that these orogens now expose terranes that were at very different crustal levels prior to deformation, it is possible to evaluate the way in which heat production is distributed in the crust. This section reviews the constraints on the distribution of heat sources in the various terranes that have been exhumed from different levels of the crust. The heat production character of the main lithostratigraphic units can be estimated using geochemical analyses and calibrated airborne radiometric data (Fig. 3). Note that heat production values listed below are quoted at 350 Ma, as appropriate to the Alice Springs Orogeny (i.e., about 6% greater than modern day values). Estimates of the characteristic thickness of the sequences derived from seismic, structural and stratigraphic studies then allows the estimation of the total thermal energy budget of the various crustal levels, which are expressed in terms of their contribution to the surface heat flow.

The crustal sections exposed in the vicinity of the Woodroffe Thrust in the Petermann

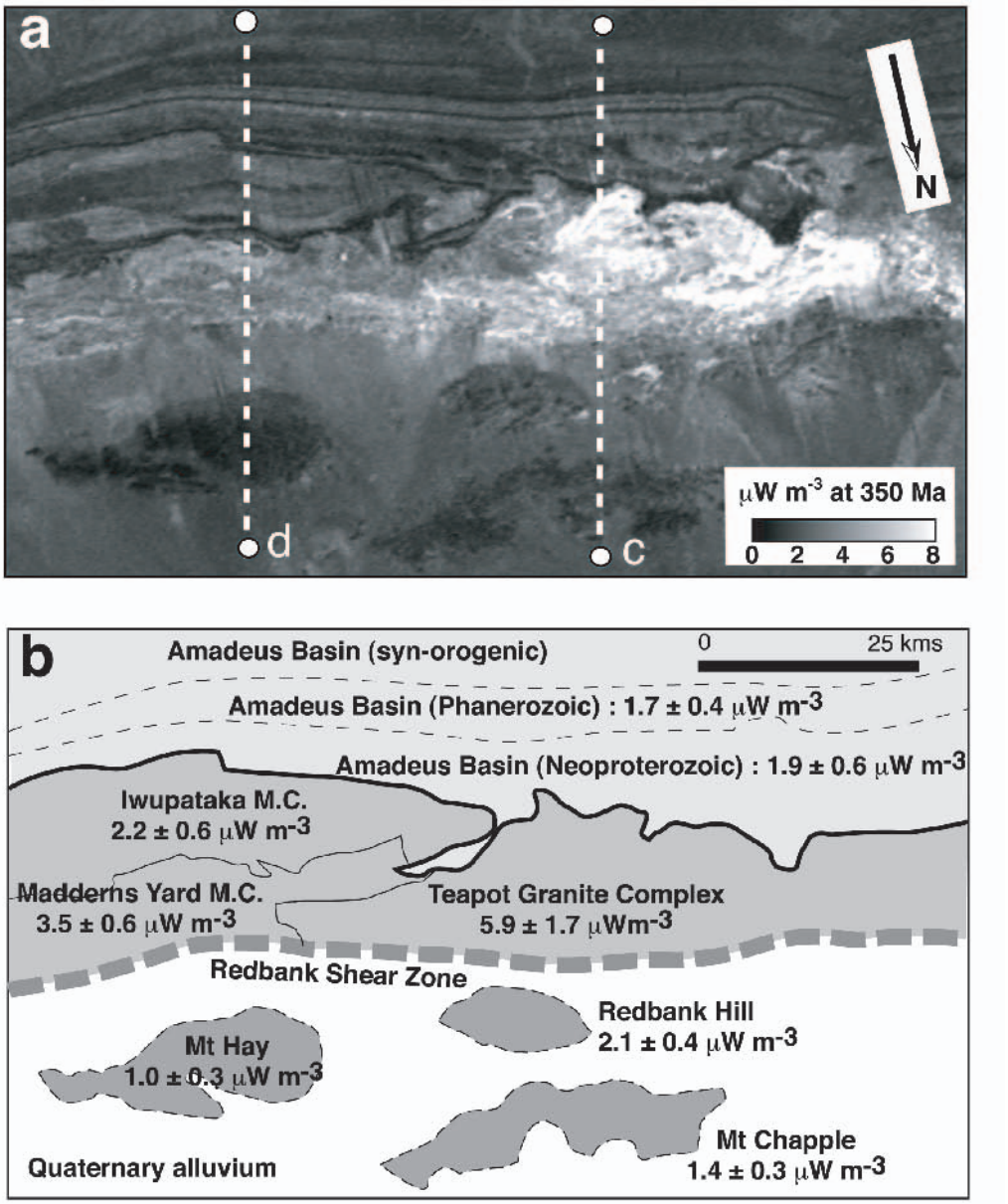

Fig. 3. (**a**) Image of heat production in the western Macdonnell Ranges (Hermannsburg Sheet) derived from Northern Territory Geological Survey airborne radiometrics. (**b**) shows the area averaged heat production rates for each of the main lithological components of this region. In the south (top), sediments of the Amadeus Basin are characterized by low-intermediate heat production rates. In the central region, high-heat producing Mesoproterozoic granites of the Teapot granite Complex, and intermediate heat producing metasediments and orthogneisses of the Iwupataka and Madderns Yard Metamorphic Complexes formed the basement upon which the Amadeus Basin sediments were deposited. North of the Redbank Shear Zone (bottom of figure), mafic and felsic granulites exhumed from the deep crust occur as isolated monadnocks (Mt Hay, Mt Chapple and Redbank Hill) surrounded by Quaternary alluvium which has largely been shed from the granites to the south. These deep crustal rocks are characterised by low-intermediate heat production rates. (**c**) heat production profile (black line) from the Ormiston Gorge region superposed with the heat production distribution (gray line) used to model heat production (equation 1). (**d**) heat production profile from the Ellery Creek region. Heat production rates are calculated at 350 Ma (i.e, during the Alice Springs Orogeny).

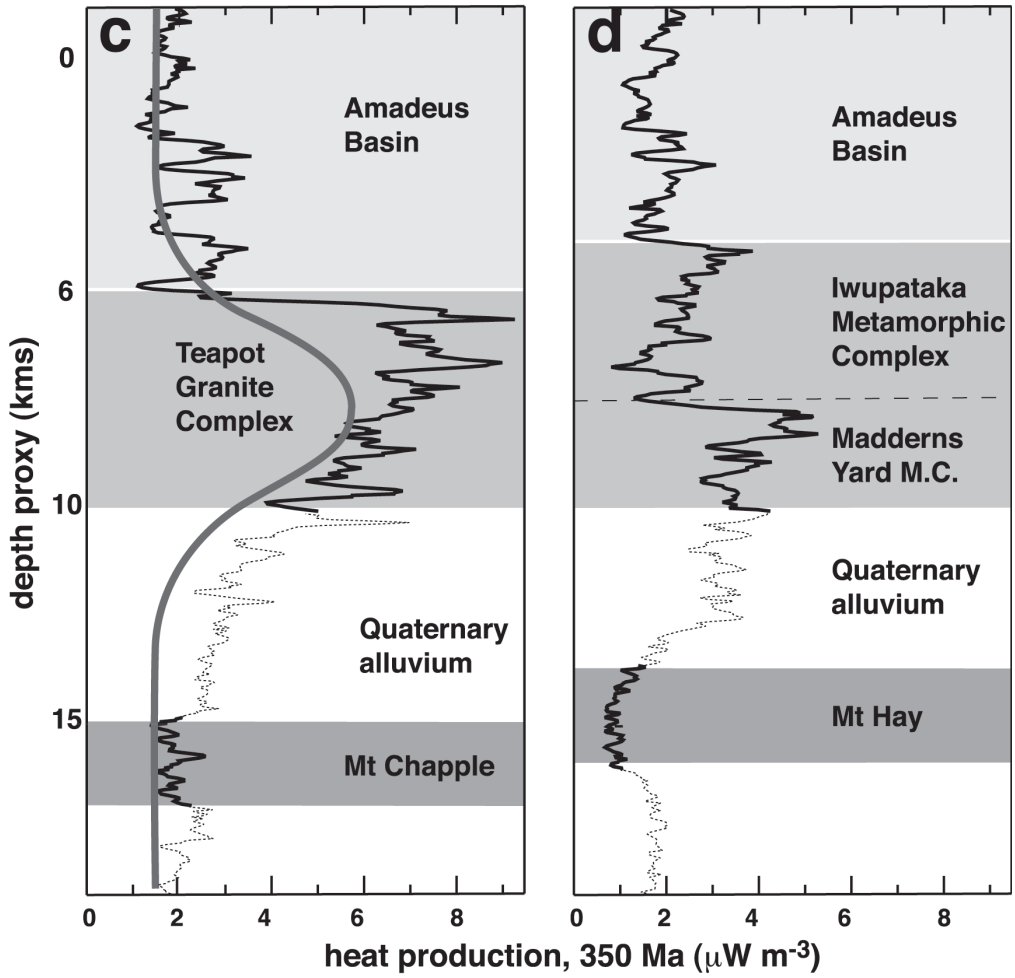

Fig. 3. (*continued*)

Orogen and the Redbank Shear Zone in the Alice Springs Orogen suggest that the central Australian crust has a relatively simple three layered structure comprising mafic to felsic lower crust, granitic and metasedimentary mid-upper crust and unmetamorphosed sedimentary upper crust (e.g. Goleby *et al.* 1989; Shaw *et al.* 1991*b*). The boundaries between these layers are generally sharp and are marked either by major shear zones or unconformities (Fig. 3).

The *mid-lower crust* is dominated by Palaeo to Mesoproterozoic mafic to felsic granulite. Modelling of gravity and seismic data suggests that this layer is between 10 and 20 km thick (Goleby *et al.* 1989; Lambeck & Burgess 1992). The heat production is typically $<2\,\mu W\,m^{-3}$ in felsic lithologies and *c.* $1\,\mu W\,m^{-3}$ in mafic rocks (Fig. 3). In the Arunta Inlier these mid-lower crustal units tend to outcrop as isolated monadnocks, prohibiting quantification of area-averaged heat production rates from the airborne radiometric data with any confidence. However, a conservative estimate of the average heat production of $1\,\mu W\,m^{-3}$ (see exposures at Mount Hay, Mount Chapple and Redbank Hill, Fig. 3a and b) implies that the mid-lower crust may contribute between about 10 and $20\,mW\,m^{-2}$ to the surface heat flow.

The *mid-upper crust* consists predominantly of Palaeo- to Mesoproterozoic metasedimentary and granitic lithologies. Gravity and seismic data, as well as baric offsets across large shear zones suggest that this mid to upper crustal layer is typically at least 10 km thick (Goleby *et al.* 1988, 1989; Warren & Hensen 1989; Lambeck & Burgess 1992). In much of the Musgrave Inlier,

this layer has been removed as a consequence of the relatively deep levels of denudation associated with the Petermann Orogeny. In the footwall of the Woodroffe Thrust, where this layer has been preserved, individual granites up to 4 km thick with outcrop extents exceeding 2000 km^2 are exposed in the cores of regional-scale antiformal culminations enclosed by cover sequences of the Amadeus Basin (Flöttmann *et al.* 1999). In the Arunta Inlier, granitic and metasedimentary lithologies dominate, reflecting the generally smaller amounts of denudation compared to the Musgrave Inlier. In the central and northern parts of the Inlier, granite accounts for up to 75% of the outcrop (Offe 1978; Wells 1982; Haines *et al.* 1991; Young *et al.* 1995). Granite heat production rates are typically greater than 5 $\mu W m^{-3}$, with some individual granite bodies contributing up to 10 $\mu W m^{-3}$ making them, by global standards, extremely effective heat producers (Sandiford & Hand 1998*b*). In the western Macdonnell Ranges (Fig. 3a), the Teapot Granite Complex averages 5.9 $\mu W m^{-3}$. The intervening metasedimentary complexes such as the Iwupataka Complex generate around 2–3.5 $\mu W m^{-3}$. The area averaged heat production rates for the mid-upper crustal zone shown in Figure 3a is 4.1 $\mu W m^{-3}$, suggesting it contributes at least 40 $mW m^{-2}$ to the surface heat flow. It is probable that there are significant spatial variations in the heat contributed by the mid-upper crust (cf. Fig. 3a, b), although the nature of the amplitude and wavelengths of such variations are not yet understood.

The *upper-most crust* consists of the sediments of the Centralian Superbasin. The sedimentary sequences are characterized by intermediate to low heat production rates. Along the northern margin of the Amadeus Basin, where the entire sequence is exposed in near vertical profile along the Macdonnell homocline, heat production varies between 0.5 and 2.5 $\mu W m^{-3}$ and averages *c.* 1.8 $\mu W m^{-3}$ (Fig. 3a, b). Together with estimates of isopachs, these heat production rates suggest that prior to each orogeny the basin contributed, at most, between 7 and 12 $mW m^{-2}$ to the surface heat flow.

Figures 3c and d show two heat production traverses across the Macdonnell Ranges from the northern Amadeus Basin to the hanging wall of the Redbank Shear Zone. This section effectively provides a depth slice through the three layered crustal structure, with 'steps' in the heat production occurring at the unconformity at the base of the Amadeus Basin, and at the Redbank Shear Zone. The profile shows that the heat production distribution immediately prior to the Alice Springs Orogeny was characterized by a pronounced maxima at palaeodepths of about 8–12 km. This distribution contrasts dramatically with the common perception that crustal heat production decreases as an exponential function of depth.

The heat production data from the central Australian region suggests that, prior to each orogeny, the average crustal contribution to the heat flow was likely to have exceeded 50 $mW m^{-2}$. In the context of global continental heat flow, especially for Precambrian terranes, this value is high (e.g. McLennan & Taylor 1996). However, it is consistent with other heat flow-heat production data from Australia. These data define an anomalous heat flow zone that includes most, but not all, of Proterozoic Australia (Cull 1982). This zone includes the eastern part of the Gawler Craton (and the adjacent Stuart Shelf), the Willyama and Mount Painter Inliers in South Australia and New South Wales, the Mount Isa Inlier in western Queensland, and the Tennant Creek Inlier in the Northern Territory (Cull 1982). The average surface heat flow in this zone is 85 $mW m^{-2}$ (Cull 1982). The zone is underlain by seismically fast and, by inference, cold and thick (>200 km) lithospheric mantle (Zielhuis & van der Hilst 1996; van der Hilst *et al.* 1998) implying mantle heat flows are unlikely to exceed *c.* 15 $mW m^{-2}$. An important implication is that the crustal contribution to the heat flow in Proterozoic Australia may be as high as 70 $mW m^{-2}$. This amounts to a lithospheric U, Th, K endowment approximately twice the continental average (e.g. McLennan & Taylor 1996), and is consistent with widespread U-mineralization through the region, including some of the largest known U-deposits (i.e. Olympic Dam).

Measured heat flow near Alice Springs is currently 60 $mW m^{-2}$ (Cull 1982) suggesting that crustal sources in the vicinity of the heat flow record currently contribute *c.* 45 $mW m^{-2}$. At Alice Springs, denudation following the Alice Springs Orogeny has removed all the cover and some of the enriched basement, while only some 10 km further north in the hanging wall of the Redbank Shear Zone both the upper and mid-crustal section has been removed. These observations suggest that the current crustal contribution to the heat flow is significantly lower than was likely to have applied immediately prior to the Alice Springs Orogeny.

Thermal aspects of heat source distribution

The analysis presented in the previous section suggests that the central Australian crust is

strongly stratified in heat producing elements, with much of the heat production concentrated in mid-upper crustal level gneissic granite terranes, where the average heat production is estimated to be at least $4\,\mu W\,m^{-3}$. Sequences both above (basin-filling sediments) and below (lower crustal gneisses) this layer, are characterized by significantly lower heat production rates. Intraplate tectonism in central Australia displaced this heat production anomaly relative to the surface. During basin formation, the high-heat producing layer was buried by up to 8 kilometres of sediment. Following intraplate orogeny, locally the layer was completely removed by erosion. While

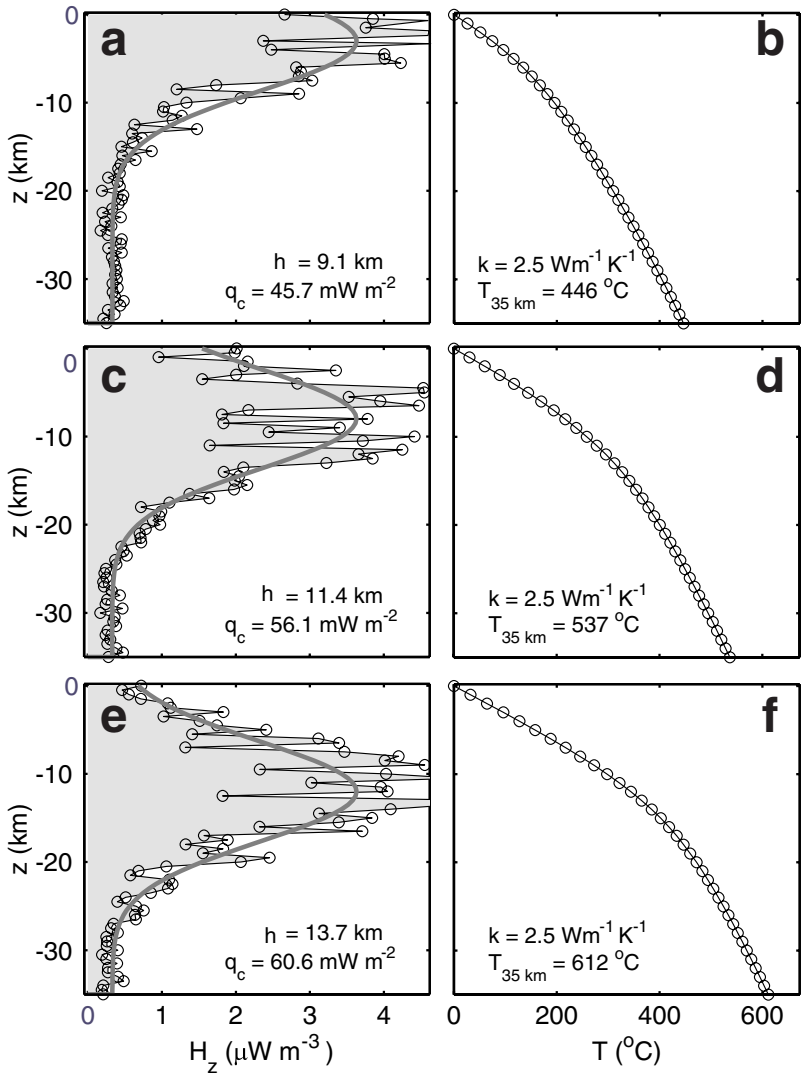

Fig. 4. Illustration of the thermal consequences of burial of an anomalous heat producing layer such as that believed to characterize the Proterozoic granitic rocks in central Australia, as shown in Figure 3. The three distributions on the left correspond to increasing depth of burial (as represented by the parameter h). Note that while the form of the heat production distribution in each is the same, and can be approximated by equation (1) as shown by the thicker solid line, the total crustal contribution to the surface heat flow q_c increases with burial due to the fact that the rocks that contribute to the burial (e.g. the sediments) add to the total heat production. The right hand side figures show the geotherms corresponding to each of the heat production distributions, and highlight the sensitivity of temperatures at depth (e.g. $T_{35\,km}$) to the depth of the heat producing layer (see Fig. 5).

the tectonic processes associated with such translation must have been associated with thermal transients it is necessary to emphasize the significant long-term thermal effects resulting from the movement of this heat source (e.g. Fig. 4). 'Long-term' implies the thermal regimes that approximate steady-state, and which applied following the dissipation of all thermal transients associated with tectonism. In so doing, we are necessarily restricting our attention to thermal consequences of processes on timescales greater than about 100 Ma. Such timescales are appropriate to the overall development of the Centralian Superbasin (which contains a depositional record spaning almost 500 Ma) and the consequences of the Petermann Orogeny during the Alice Springs Orogeny, some 100–200 Ma later.

In order to quantify the long-term thermal consequences of such vertical translation it is useful to approximate the distribution with an analytic function. Following Sandiford & Hand (1998*b*), the distribution of heat production in central Australia is approximated as an exponential function which attains a maximum H_i at a discrete level z_i within the crust (Fig. 3b):

$$H(z) = H_i \exp\left(\frac{-(z - z_i)^2}{h_r^2}\right) \tag{1}$$

In equation (1) the parameter h_r provides a measure of the spread of the heat production distribution with the heat production falling to $H_i e^{-1}$ at depths $z_i \pm h_r$. Subject to a basal heat flow, q_m, applied at a depth beneath which heat production is negligible and the heat production distribution in equation (1) the resulting temperature field is:

$$\begin{aligned} T(z) = &-\frac{q_m z}{k} + \frac{H_i h_r^2}{2k}\left(\exp\left(-\frac{z_i^2}{h_r^2}\right)\right. \\ &\left. - \exp\left(-\frac{(z_i - z)^2}{h_r^2}\right)\right) + \frac{h_r H_i \sqrt{\pi}}{2k} \\ &\times \left(z\,\mathrm{Erf}\left(\frac{z_c - z_i}{h_r}\right) + (z_i - z)\,\mathrm{Erf}\left(\frac{z - z_i}{h_r}\right)\right. \\ &\left. + z_i\,\mathrm{Erf}\left(\frac{z_i}{h_r}\right)\right) \end{aligned} \tag{2}$$

where k, is the thermal conductivity assumed to be both temperature and depth independent. Note that the 1-D approximation in equation (2) implies no lateral variations in heat production parameters. Figure 3 clearly shows significant lateral variation in heat production in the high-heat producing granitic layer. In choosing parameters relevant to central Australia it is therefore important to use average, rather than extreme, parameters. In the following, heat production parameters contribute a total of $45\,\mathrm{mW\,m^{-2}}$ to the surface heat flow with a maximum heat production of $4\,\mu\mathrm{W\,m^{-3}}$, thus constraining the characteristic length scale h_r to be *c.* 7 km. In view of our earlier discussion this is a rather conservative estimate of the contribution made by crustal sources in this region.

In the following section the long-term thermal consequences of the burial of such a heat-producing layer, by calculating the changes in the temperature at deep crustal- upper mantle depths accompanying erosion and/or sedimentation are explored. Figure 5a shows that the erosional removal of the sedimentary cover from this heat producing layer will lead to long-term cooling of the Moho by about *c.* 18°C per kilometre of denudation for parameter ranges appropriate to central Australia. Note that this estimate is sensitive to the value of the mantle heat flux and the thermal conductivity, which together determine the thermal gradient in the deeper part of the lithosphere, both of which are relatively poorly constrained. Approximately half the Moho cooling is due to shallowing of the Moho, while the remainder is due to deep crustal cooling in response to the change in the depth of the heat producing layer.

The evaluation of the long-term thermal effects of the burial of such a sequence beneath an accumulating sedimentary pile requires an understanding of the factors that contribute to subsidence (e.g. Sandiford 1999). If the pre-existing crust is simply buried beneath the sedimentary pile such that the whole crust including the Moho is displaced, then the long-term Moho temperature will be the opposite of that induced by erosion (i.e. for $q_c = 45\,\mathrm{mW\,m^{-2}}$, Moho temperatures increase by about $18^\circ\mathrm{C\,km^{-1}}$ of basin-fill). However, more typically basin formation is induced by crustal stretching and the Moho displacement will not be directly coupled with the thickness of the sedimentary basin. Moreover, crustal stretching will attenuate pre-existing crustal heat production. As discussed by Sandiford (1999), the thermal consequences of this style of basin formation will reflect a competition between burial of the pre-existing heat production, which tends to heat the crust, and the attenuation of the pre-existing heat production, which tends to cool the crust. Figure 5b shows that for the case where the total subsidence is sufficient to preserve the Moho at its pre-stretching depth, then Moho temperatures will rise about 9°C for each kilometre of subsidence. In a more typical case, where the Moho shows long-term shallowing as a consequence

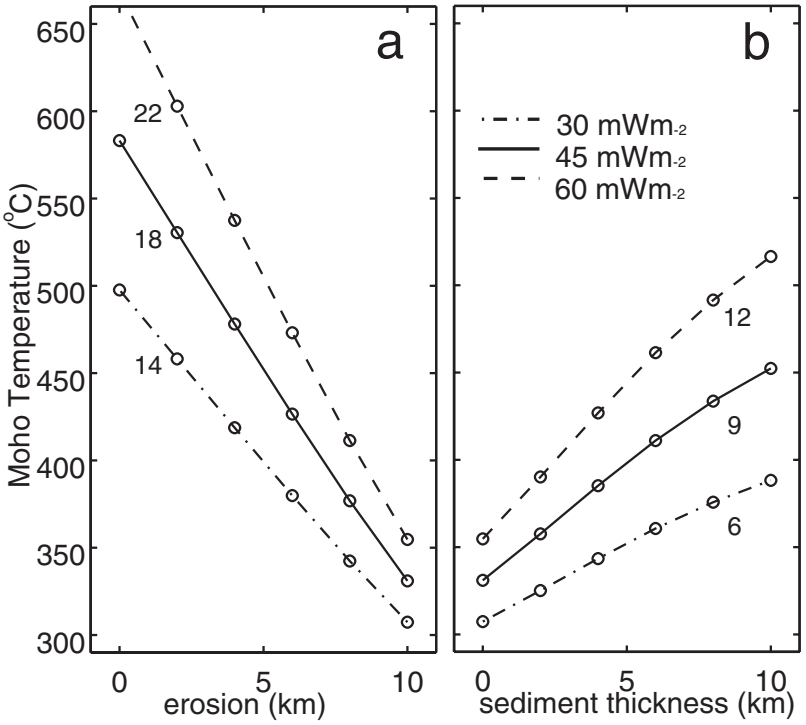

Fig. 5. Illustration of the long-term thermal effects of (**a**) exhuming a central Australian like heat production distribution from beneath a thick sedimentary succession such as the Centralian Superbasin, and (**b**) burying it beneath a sedimentary succession, where the subsidence is related to crustal stretching (see text for discussion). Three different curves represent three different total abundances of heat producing elements, i.e. $q_c = 30$, 45, and $60\,\mathrm{mW\,m^{-2}}$. For Central Australia, we estimate q_c is on average at least $45\,\mathrm{mW\,m^{-2}}$. The numbers on each curve indicate the magnitude of the change in Moho temperature per kilometre of denudation/burial. Other model parameters are $q_m = 20\,\mathrm{mW\,m^{-2}}$, $k = 3\,\mathrm{W\,m^{-1}\,K^{-1}}$. Increasing q_m and/or decreasing k will tend to increase the magnitude of the thermal response to denudation/burial.

of rifting, Moho temperatures may in fact be reduced (e.g. Sandiford 1999). However, even for cases where the Moho is cooled because of such shallowing, the temperature at any given depth will inevitably increase due to the thermal consequences of the burial of the heat-producing layer (see below).

A generalized model for heat production changes during intraplate deformation

In the previous section it was demonstrated that changes in the heat production distribution have a profound effect on the thermal structure in the deep crust and upper mantle. This can be generalized using a simple parameterization of crustal heat production involving just two parameters: the vertically-integrated crustal heat production, q_c, and the characteristic length scale for heat production, h. Formally, q_c and h are defined as follows:

$$q_c = \int_0^{z_c} H(z)\,dz \tag{3}$$

$$h = \frac{1}{q_c}\int_0^{z_c} (H(z)z)\,dz \tag{4}$$

Importantly, this definition of h makes no explicit assumption about the form of the heat production distribution. h, can be thought of as the e*ffective depth* of the heat production distribution (Fig. 6). Physically, it can be understood as the depth at which concentrating all q_c heat sources (i.e., as a delta spike) does not alter the thermal structure at or beneath the base of the crust. The parameterization of the crustal heat production distribution in terms of h and q_c has a number of benefits. Firstly, it allows

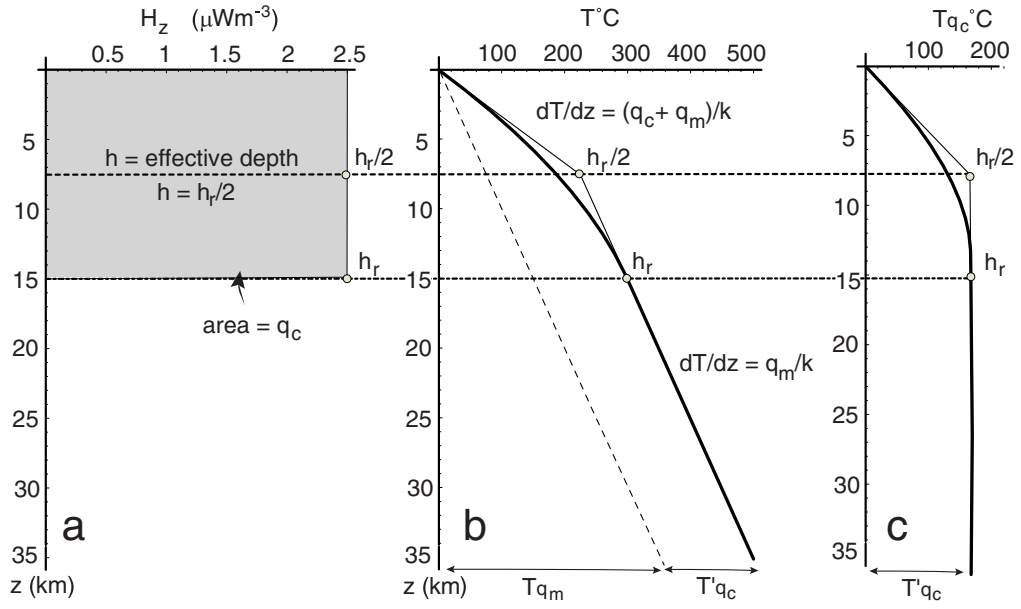

Fig. 6. Illustration of the effect of a heat source distribution (**a**) on the temperature field shown by the thick solid line in (**b**). The dashed line in (**b**) represents the contribution of mantle heat flow. The difference between the actual temperature field and the mantle contribution is a measure of the crustal heat source contribution, T_{q_c}, as shown in (**c**). T_{q_c} attains a maximum value T'_{q_c} ($= hq_c/k$) at the base of the heat producing layer (i.e. depth h_r). The parameter h represents the *effective depth* of the heat production. For the heat source distribution consisting of a layer of thickness h_r with uniform heat production, the effective depth $h = h_r/2$. Concentrating all q_c heat sources as a delta spike at depth h does not affect the value of T'_{q_c} (as shown by the thin solid line in (**b**) & (**c**) which shows the temperature field for such a distribution).

the effects of tectonic processes to be quantitatively portrayed on the h–q_c plane. Secondly, the contribution of crustal heat sources to the temperature field at or beneath the base of the heat producing parts of the lithosphere (i.e. the Moho) can be expressed succinctly as a linear function of both h and q_c:

$$T'_{q_c} = \frac{q_c h}{k} \tag{5}$$

T'_{q_c}, can be considered as the thermal contribution caused by the heat source distribution relative to an otherwise identical lithosphere with no heat production (Fig. 6). The long-term consequences of tectonic processes on the heat production parameters of the crust can be illustrated using a simple scenario appropriate to crustal stretching and basin formation (Fig. 7). Normally continental extension is accompanied by basin formation with associated subsidence continuing for up to *c*. 100 Ma as thermal transients induced by the extension are dissipated. In order to provide a clear picture of the combined effects of crustal stretching and basin formation on the heat production distribution we treat them sequentially. Figure 7a shows a crust initially 30 km thick, with a simple heat source distribution consisting of an upper crustal layer some 15 km thick characterized by an uniform heat production ($3\,\mu W\,m^{-3}$) beneath which heat production is assumed to be negligible. This crust is therefore characterized by a total (vertically-integrated) heat production of $45\,mW\,m^{-2}$. For this distribution, the appropriate length scale that conforms to equation (4) is given by the mean depth of the heat production, i.e. $h = 7.5$ km (see Appendix 1 for further details). From equation (5), $T'_{q_c} = 112°C$ ($k = 3\,W\,m^{-1}\,K^{-1}$). A stretching event which homogeneously attenuates the crust to 2/3 its original thickness (Fig. 7b) reduces q_c to $30\,mW\,m^{-2}$, h to 5 km and T'_{q_c} to 50°C. If allowed to thermally equilibrate temperatures at any depth below the heat producing layer would cool by 62°C as the direct consequence of the changes in the heat production distribution. Note that because of the 10 km reduction of the Moho depth inherent in this scenario there would be significant additional cooling of the Moho or any other

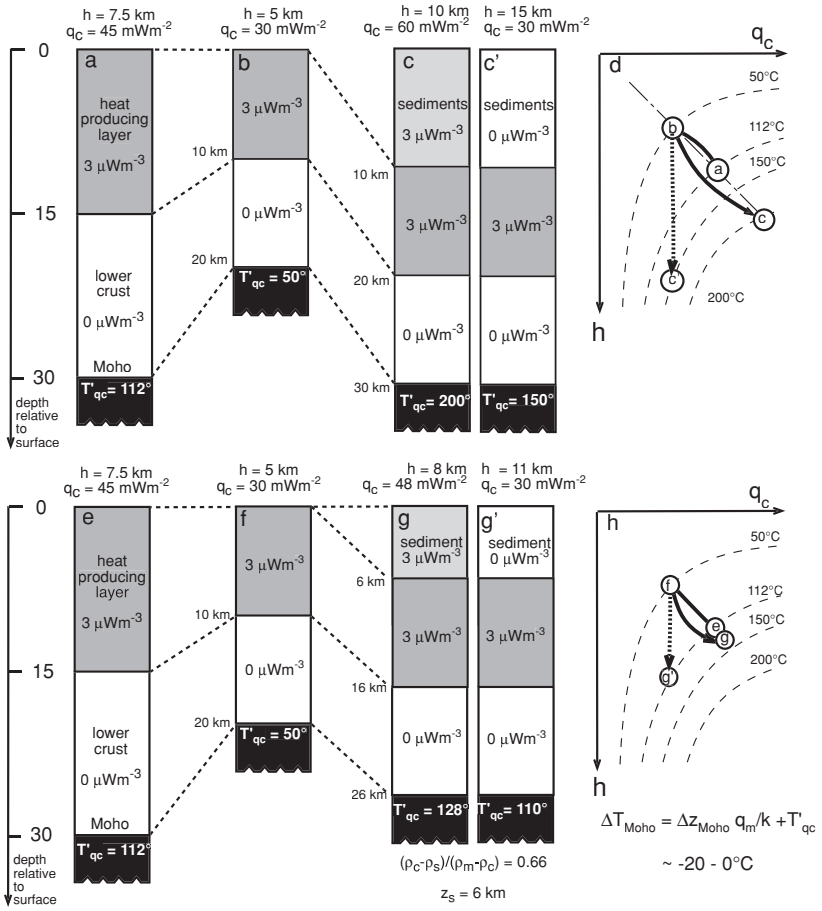

Fig. 7. Schematic illustration of the way in which crustal stretching and associated basin filling change the heat production parameters in the crust (a more detailed account of the long-term thermal consequences of basin formation is given by Sandiford 1999). Column (**a**) illustrates the reference state prior to crustal stretching, and the numbers along side the Moho in each column, represent the contribution of heat sources to the temperature field at that depth (i.e. T'_{q_c}), if the column were left to thermally equilibrate as illustrated. The long-term changes in the temperature of the Moho contributed by changing heat source distributions are given by the change in T'_{q_c} following a tectonic process. For this scenario, the combined effects of crustal stretching (**b**) and basin filling with heat-producing sediments (**c**) result in a long-term heating of the Moho by 88°C. The thermal effects are dependent on thermal properties of the basin filling sediments. However, even in the case where basin filling sediments contain no heat production (**c′**) there is a long-term increase in Moho temperature of 38°C. (**d**) shows that the various scenarios can be represented on the h–q_c plane (see also Fig. 8). Figure 7c applies when the density of the basin-fill is similar to the pre-existing crust. However, even when sediments are less dense, and the basin therefore less deep $\Delta T'_{q_c}$ may be positive (Fig. 7e–f). Note however, that in this case the long-term shallowing of the Moho will mean that $\Delta T_{\mathrm{Moho}} < \Delta T'_{q_c}$ (see Sandiford 1999).

material point beneath the base of the heat producing layer. The effect of filling the accommodation space created by extension with sediments depends on the properties of the sediments. If the sediments have heat production rates comparable to the pre-existing upper crust (i.e. $3\,\mu\mathrm{W\,m^{-3}}$) and are sufficiently dense that in filling the basin the Moho is displaced back to its original depth (Fig. 7c), the resulting heat producing layer would be some 20 km thick (comprising a 10 km thick basin together with the 10 km thick attenuated pre-existing heat producing layer) and would contribute $60\,\mathrm{mW\,m^{-2}}$ to the surface heat low. In this scenario (h is 10 km, T'_{q_c} is 200°C), the combined effects of stretching and sedimentation yield a change in T'_{q_c} of

c. 88°C, or about 9°C/km of sediment-fill (cf. Fig. 5b). While the long-term thermal response is sensitive to the heat production contributed by the sediments, there maybe a long term increase, albeit small, in T'_{q_c} even when the sediment-fill contains no heat production (Fig. 7c). This highlights the fact that the long term thermal response to extensional basin formation reflects a competition between attenuation (leading to cooling) and burial (leading to heating) of the pre-existing heat production. Where the density of the basin-filling sediments is somewhat less than the crustal average, isostasy dictates a long-term shallowing of the Moho, possibly by as much as 4 km for the stretching scenario outlined above depending on the density of the sediment, with a correspondingly smaller T'_{q_c} (Fig. 6e–g). Moreover, the shallowing of the Moho in this scenario causes additional Moho cooling (by approximately $q_m \Delta z/k$, where Δz, is the amount of Moho shallowing), implying that even though $\Delta T'_{q_c}$ may be positive (i.e. long-term heating at a specific depth), ΔT_{Moho} may be negative (i.e. long-term cooling of the Moho). A more detailed analysis of the long-thermal consequences of rift basin formation is given by Sandiford (1999).

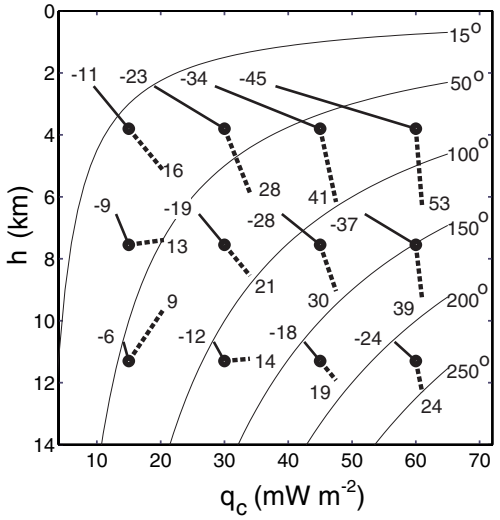

Fig. 8. With a suitable chosen length scale (equation 3, Appendix 1), the long term thermal consequences of a tectonic process can be predicted from the associated changes in h and q_c, allowing portrayal on the h–q_c plane. The bold lines show the effects of the imposition of a 10% stretch with associated basin filling (*c.* 3.5 km) on q_c and h. The thin lines show the effects of a 10% crustal shortening, followed by erosion (*c.* 3.5 km) back to the pre-shortening crustal thickness. The initial geometry, indicated by the bullet points, consists of an upper crustal layer of thickness $2h$ characterized by a uniform heat production of magnitude $q_c/(2h)$. Note that for a given crustal strain the most dramatic changes in temperature are expected when the crust is already strongly stratified in heat producing elements, and unusually enriched (i.e. low h and high q_c), as appears to be the case for the central Australian crust. In contrast, the processes are rather less effective when operating on crust which shows no substantial differentiation of heat producing elements (e.g. large h). In this modelling, basin-filling sediments are assumed to contribute 2 μW m^{-3}, while the conductivity is assumed to be 3 Wm^{-1} K^{-1}.

The above analysis shows that the long-term thermal consequences of tectonic processes relate directly to the way these processes change h and q_c. Figure 8 uses these two parameters to illustrate the thermal consequences of basin formation (dashed lines) induced by a 10% crustal stretch for the case where the basin filling sediments (*c.* 3 km) have only half the heat production of the upper crust. Also shown, in solid lines is the effect of a 10% homogeneous shortening of the crust, followed by erosion such that crustal thickness returns to its original (pre-shortening) value. Although a 10% strain at the crustal scale represents only a very mild deformation, Figure 8 shows that, when coupled with an associated surface response such as erosion, such deformations can result in very substantial redistribution of crustal heat sources. This in turn has profound consequences for the long-term thermal state of the lithosphere. In general, crustal stretching and basin formation will lead to long-term heating at deep crustal and upper mantle levels, while crustal shortening and associated erosion leads to long-term cooling (note that the Moho may experience additional changes in temperature if its depth is also changed). For a given crustal strain, the most dramatic changes in temperature are expected when the crustal heat production distribution is already strongly differentiated, and unusually enriched (i.e. low h and high q_c), as appears to be the case for much of the Australian Proterozoic crust including central Australia. In contrast, the processes are rather less effective when operating on relatively undifferentiated crust (i.e. large h).

Mechanical consequences of heat source redistribution

Emphasis has been placed on the long-term thermal consequences of burial and denudation in central Australia, as reflected in thermal regime in the deep crust and upper mantle. Primarily because the upper mantle temperatures are likely to provide a useful proxy for lithospheric strength

(e.g. Sonder & England 1986). In this section an attempt to quantify how such long-term thermal changes might change the strength parameters of the lithosphere using a 'Brace-Goetze' rheology in which the lithosphere is assumed to deform by a combination of frictional sliding and ductile creep (e.g. Brace & Kohlstedt 1980). The application of the 'strength envelope' approach implicit in this 'Brace-Goetze' rheology has become widespread in geodynamic problems, and is now very familiar. However, such calculations are highly uncertain (e.g. Paterson 1987), because:

- the extrapolation of rheological flow laws from laboratory conditions and timescales to the geological realm involves many orders of magnitude;
- our imprecise understanding of the compositional and mineralogical structure of the lithosphere translates to uncertainties in knowledge of what particular flow law applies in any given part of the lithosphere; and
- our imprecise knowledge of the thermal property structure of the lithosphere (particularly thermal conductivity) results in considerable uncertainty in its absolute thermal structure.

These problems render any calculation of absolute strength rather pointless, and in the following section emphasis is placed on relative changes in lithospheric strength that accompany changes in the thermal structure of the lithosphere as a consequence of changes in the heat production parameters. While the precise magnitude of these relative strength changes will depend on the composition and thermal structure of the reference frame, they are likely to be far more robust than any absolute measure of strength, because most of the uncertainties alluded to above will cancel.

In previous sections it has been demonstrated that changes in heat source distribution, associated with tectonic processes affecting the central Australian crust, produced long-term changes in Moho temperatures of the order of 100°C. The greatest changes are likely to be due to erosional denudation of deep crustal rocks in the cores of the orogens. Figure 9 shows how such changes in crustal thermal structure accompanying such denudation impact on the strength. In constructing Figure 9 we have used strength parameters appropriate to quartz-dominated upper crust (sedimentary succession), feldspar-dominated mid-lower crust, and olivine-dominated mantle (see Sandiford *et al.* 1988, for a more detailed account). For the parameters used in the calculation of Figure 9 ($q_c = 45\,\mathrm{mW\,m^{-2}}$, $k = 2.5\,\mathrm{W\,m^{-1}\,k^{-1}}$, $q_m = 25\,\mathrm{mW\,m^{-2}}$), 5 km of denudation (i.e. *c.* 90°C Moho cooling; Fig. 8) leads to sufficient strengthening of the system to reduce effective strain rates by *c.* four orders of magnitude. These calculations highlight the

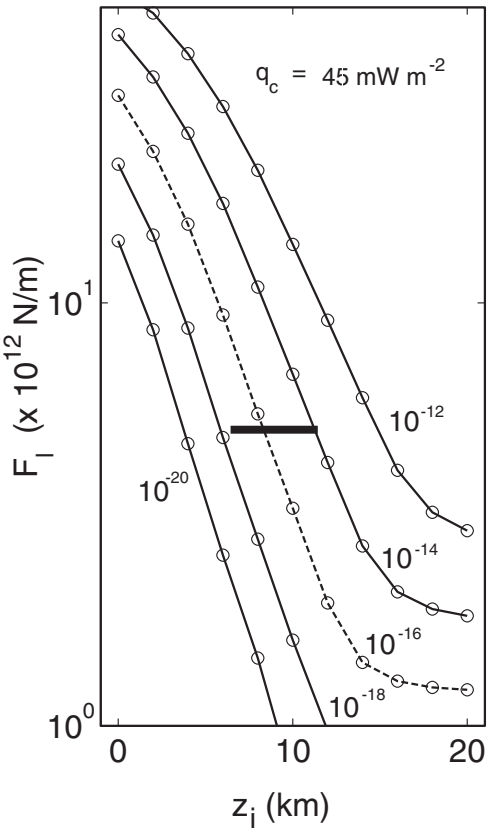

Fig. 9. Illustration of the rheological effects of progressive denudation of a radioactive basement using a 'Brace-Goetze' rheological model as discussed in the text, and the thermal parameter range used in Figure 5. The parameter z_i represents the locus of maximum heat production. In terms of the central Australian example, it corresponds to a depth several kilometres beneath the basement-cover unconformity. The calculated lithospheric strength (F_i) is shown for a range of effective strain rates ($= 10^{-12}$, 10^{-14}, 10^{-16}, 10^{-18} and $10^{-20}\,\mathrm{s^{-1}}$). The strength parameter (F_i) can be best viewed as the magnitude of the tectonic force driving deformation. At $F_i = 5 \times 10^{12}\,\mathrm{N\,m^{-1}}$ a decrease in the burial of the basement sequence by 5 km results in a corresponding decrease in strain rate of up to four orders of magnitude (solid bar), provided thermal equilibration takes place. Note that while the absolute values of the calculated strain rates at any given strength (or strengths at a given strain rate) are highly uncertain, rather more confidence is attached to estimates of the relative changes that accompany a given change in the thermal state.

extraordinary temperature sensitivity of the 'Brace-Goetze' lithosphere, particularly given that the rates of geologically-significant distributed tectonic deformation in the modern continents spans little more than about four orders of magnitude.

Recognizing that the h–q_c plane can be contoured for thermal structure (Fig. 8) allows it to be contoured for changes in strength parameters (Fig. 10), with the proviso that the tectonic processes that lead to alteration in the heat production parameters do not also lead to long-term changes in the depth of the Moho (see below). In Figure 10, the mechanical response has been normalized against the reference frame, characterized by an initial configuration with $q_c = 45\,\mathrm{mW\,m^{-2}}$ and $h = 7.5\,\mathrm{km}$, to emphasize relative changes in strength parameters. Figure 10a shows the change in strength at a specified strain rate. Note that the stretching – basin filling scenario illustrated in Figure 7a–c results in a two-fold variation in lithospheric strength. While strength envelope calculations are often presented as effective strength at a given strain rate (e.g. Fig. 10a), it is probably more useful to consider the rate of deformation that would apply as a result of an imposed force. Figure 10b illustrates the (normalized) deformation rates in response to an imposed tectonic force of $5.3 \times 10^{12}\,\mathrm{N\,m^{-1}}$. The stretching-basin filling scenario illustrated in Figure 7a–c results in an effective change in rate of deformation of *c.* 1–2 orders of magnitude.

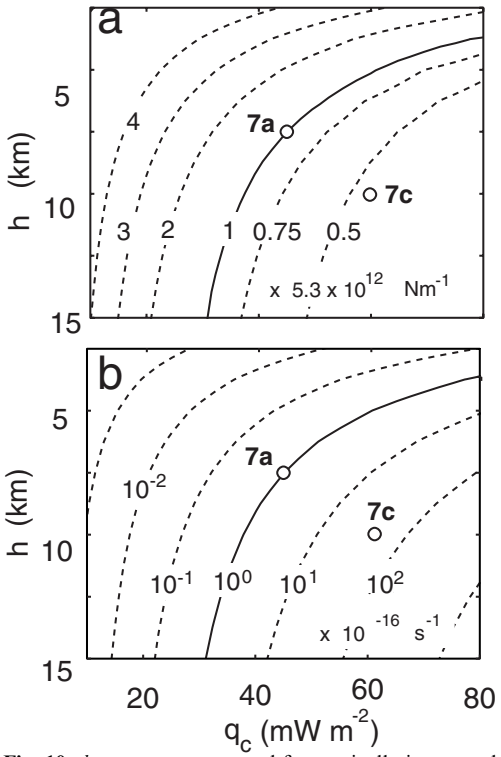

Fig. 10. h–q_c space contoured for vertically-integrated strength normalized against a lithosphere with $h = 75\,\mathrm{km}$ and $q_c = 45\,\mathrm{mW\,m^{-2}}$ (i.e., the notional central Australian lithosphere). Figure 10a shows variations in the normalized strength at a constant strain rate ($10^{-16}\,\mathrm{s^{-1}}$). The estimated strength of the reference lithosphere is $5.3 \times 10^{12}\,\mathrm{N\,m^{-1}}$. Figure 10b shows the strain rate that would apply to a lithosphere subject to a tectonic force of $5.3 \times 10^{12}\,\mathrm{N\,m^{-1}}$. It should be noted that these estimates are dependent on the assumed compositional and rheological properties of the lithosphere. It is emphasized that these calculations are based on the assumption that there is no long-term change in Moho depth, as might be expected following extensional deformation and basin formation (see Sandiford 1999). Points 7a and 7c correspond to points (**a**) and (**b**) in Figure 7.

The calculations summarized in Figures 4–9 highlight an important and often overlooked aspect of continental rheology; namely, the rheological properties of the lithosphere are not time invariant, as is often implicitly assumed. Most importantly, the evolution of lithospheric strength is dependent on past tectonic activity. The calculations summarized here suggest that the amplitude of such time-dependent strength variations in continental interiors is large, and may be of similar magnitude to the spatial variations in strength arising from variations in the compositional make-up of the lithosphere. Our purpose in Figures 4–9 has been to highlight the role played by heat production distributions in modulating the long-term strength of the lithosphere. It must be noted, however, that Figure 10 only applies when Moho depth is held constant. As pointed out by Braun (1992) and Sandiford (1999), tectonic processes such as crustal extension leading to basin formation also typically lead to long-term changes in the depth of the Moho because they affect the density structure of the lithosphere. Changes in the depth of the Moho will also affect the strength of the lithosphere and therefore are also critical to the interplay between tectonism and long-term lithospheric strength.

2-D considerations

Our analysis of the thermal consequences of tectonic process that change heat source distribution has so far been 1-D. Such an analysis is only applicable if the processes operate on horizontal length-scales that are of similar order,

or greater, than the thickness of domain over which conduction is occurring. In this case the thickness of the lithosphere defines the appropriate domain. In central Australia, the lithosphere is of the order of 200 km thick (Zeilhaus & van der Hilst 1996). While the broad depocentres associated with regional variations in isopach geometry within the Centralian Superbasin are of this order, the subsequent basement uplifts, and particularly the domains in which deep crustal rocks have been exhumed are rather narrower. For example, the width of the mafic granulite domains in the cores of both the Musgrave and Arunta Inliers is *c.* 30–50 km (Fig. 1). In this section the role geometry plays in modulating the thermal response to the localized redistribution of a heat sources in 2-D is considered, focussing particularly on the long-term cooling associated with basement uplifts such as the Musgrave and Arunta Inliers.

To do this a variation of the heat production distribution used for the 1-D case examined is adopted to describe a spatially localized heat production anomaly:

$$H(x,z) = H_{\mathrm{i}} \exp\left(\frac{-(z-z_{\mathrm{i}})^2}{hz_{\mathrm{r}}^2}\right) * \exp\left(\frac{-x^2}{hx_{\mathrm{r}}^2}\right) \quad (6)$$

where hz_{r} and hx_{r}, are the characteristic length scales of the heat production anomaly in the vertical and horizontal directions, respectively. Figure 11 shows the temperature variation (normalized against the solution for the 1-D approximation) directly beneath the centre of the heat production anomaly as a function of the parameter hx_{r} (the characteristic horizontal length scale). The calculations summarized in Figure 11 indicate that providing the characteristic length scale of the heat production anomaly is greater than about 50 km, then upper crustal temperatures will be greater than 50% of the 1-D approximation. Figure 11 also shows that for any given value of hx_{r}, the normalized temperature decreases with increasing depth. At Moho depths (i.e. 30–35 kms) it is *c.* 15% lower than at 10 km depth. In view of the importance of Moho temperature in dictating the strength of the lithosphere, these calculations inform us about the horizontal scales in heat production distribution in the mid-upper crust required to produce significant mechanical effects. The across-strike dimensions greater than about 50 km are required in order for sub-basins, or subsequent uplifts, to seriously perturb lithospheric thermal structure at Moho levels. In central Australia, the sedimentary cover has been removed from the basement inliers over many hundreds of kilometres, while very deep levels of denudation in the cores of the inliers have characteristic across strike widths of *c.* 50 km. Consequently, the effective temperature changes at Moho levels are likely to be at least 50% of the estimate derived from the 1-D estimates (i.e., for central Australian heat production parameters about 9°C/km of erosion).

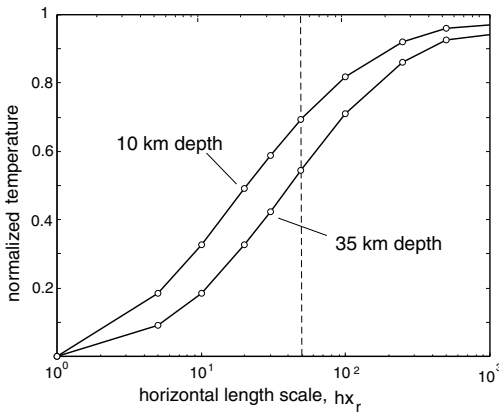

Fig. 11. In order to illustrate the effect of the horizontal length scale for the heat production anomaly, we show the temperatures at depths $z = 10$ and 35 km beneath the surface of an anomaly as a function of horizontal length-scale of the anomaly, hx_{r} (see text for discussion). The temperatures are normalized against the solution for the 1-D (infinite sheet) approximation, and thus span a range from 0 at $hx_{\mathrm{r}} = 0$ (i.e., no anomalous heat production) to 1 at $hx_{\mathrm{r}} = \infty$ (i.e. the 1-D solution).

Rates of deformation and the mechanics of intraplate orogens

Previous sections have shown that tectonic processes, such as basin formation, deformation and erosion, have played a profound role in geochemically structuring the crust in the central Australian region. Moreover, the redistribution of heat production as a consequence of these processes has had profound long-term thermal consequences. Given our current understanding of the rheology of the lithosphere, these changes are likely to have profoundly affected its mechanical structure. The motivation for this analysis has been the unusual spatial and temporal patterns of deformation associated with intraplate deformation in this region. This distribution suggests that the strength parameters of this region have varied both in space and time in very significant ways. If this analysis is correct it raises the intriguing possibility that the changes in

strength induced by this geochemical structuring have influenced the progression of ongoing deformation during the orogenic cycle. This section addresses this question using constraints on the duration, and rates, of deformation during the Alice Springs Orogeny. Particular interest is placed on relating this question to the origin, and long-term preservation, of the extraordinary gravity anomalies (Mathur 1976) that seem to be the hallmark of the central Australian intraplate orogenies. The Redbank Shear Zone is used as a prototype for the style of deformation associated with these orogenies.

The Redbank Shear Zone is a well-defined crustal-scale structure that can be traced on seismic profiles (Goleby *et al.* 1988, 1989) to depths of at least 40 km, where it clearly displaces the Moho by about 15 km. The crust is effectively ramped up along this *c.* 45° dipping segment of the Redbank Shear Zone such that it is now deeply denuded in the hanging wall of the structure (Fig. 13). It seems unlikely that such ramping could continue to much deeper levels than about 40 km, where displacement might be expected to be accommodated on shallowing detachments, or alternatively, partitioned into a corresponding downward directed flow in the deeper mantle (e.g. Braun & Shaw 1998; Fig. 13). The horizontal displacement of the Redbank Shear Zone and its associated splays such as the Ormiston Thrust during the Alice Springs Orogeny has recently been estimated at

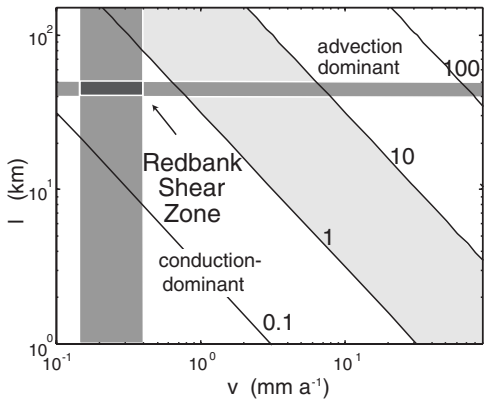

Fig. 12. Estimated values of mean displacement rates, *v* and appropriate length scales, *l*, for the movement on the Redbank Shear Zone during the Alice Springs Orogeny. Contours show values of thermal Peclet numbers, Pe_T, and indicate that the Alice Springs Orogeny operated in a regime where conduction was likely to dominate its thermal evolution. Note that typical plate margin orogenies evolve with $Pe_T \gg 10$.

20 km (Flöttmann & Hand 1999). While precise constraints on the duration of activity on the Redbank Shear Zone are not available, the maximum bound on the duration of the Alice Springs Orogen of 150 Ma provides a time-averaged lower bound on the displacement rate of *c.* 0.125 mm a^{-1}. An upper bound on the time-averaged displacement rate of *c.* 0.4 mm a^{-1} is provided by the evidence that sediment was shed from the hanging wall of the Redbank Shear Zone for at least 50 Ma, from *c.* 390–340 Ma (Shaw *et al.* 1991*a*).

While the history of displacement on the Redbank Shear Zone may well have been intermittent within these intervals, these bounds do provide an insight into the thermal response of the system to active deformation and denudation. In essence we are interested in whether the conductive response to changing heat source distributions overlap with the ongoing deformation. The qualitative thermal response of a deforming system is encapsulated in the thermal Peclet number, Pe_T, which provides a measure of the rate of advection of heat to conduction of heat (Fig. 12):

$$Pe_T = vl/\kappa \tag{7}$$

where *v*, is the characteristic velocity; *l*, is the appropriate length scale; and κ, is the thermal diffusivity. For $Pe_T > 10$, heat is carried with the deformation and so advection dominates the thermal evolution, whereas for $Pe_T < 1$ conduction dominates the evolution. Using the averaged displacement rates discussed above for the Redbank Shear Zone, where *l* is *c.* 40 km, κ *c.* 10^{-6} m^2 s^{-1}, we estimate Pe_T to be *c.* 0.1–0.4, suggesting conductive heat transfer dominated the thermal evolution during deformation.

The notion that the Alice Springs Orogen evolved in a regime in which conduction dominated its ongoing thermal evolution is important. Plate margin orogens typically evolve at high Pe_T numbers because of the governing role played by subduction. The inference that the Alice Springs Orogen evolved at a low Pe_T raises the possibility that its mechanical evolution may have differed from the somewhat more familiar plate margin orogens. In particular, it raises the possibility that the cooling associated with exhumation of low-heat production deep crustal rocks during ongoing deformation has led to sufficient lithospheric strengthening to stall the deformation by providing a kind of 'thermal lock'. In order to constrain the thermal evolution during movement on the Redbank Shear Zone, a straightforward kinematic model has been used for deformation, as illustrated in Figure 13. The

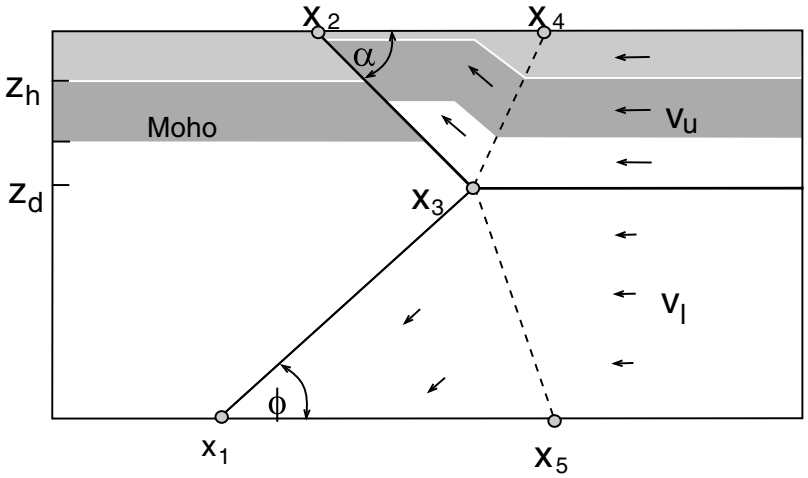

Fig. 13. Kinematic model for intraplate deformation on the Redbank Shear Zone during the Alice Springs Orogeny, based on the models of Beaumont *et al.* (1994). In this model the Redbank Shear Zone is assumed to sole at depth z_d slightly below the Moho. Displacement of the upper plate above the detachment occurs at rate v_u while a corresponding flow at rate v_l in the deeper mantle takes material down. See Figure 14 for details of thermal structure resulting from displacement at various values for v_u and v_l. Displacement causes the exhumation of an upper crustal heat producing layer, with erosion assumed to keep pace with deformation such that no substantial topography is generated during ongoing deformation.

results are shown in Figure 14. Two different scenarios have been explored, which apply to different behaviours in the deeper mantle lithosphere. In the first case it is assumed that mantle lithosphere shortens at the same velocity as the crust, inducing a singularity in the velocity field at x_3 (this follows closely from the models of Beaumont *et al.* 1994). In the second case it is assumed there is no deformation of mantle material at least in the vicinity of the crustal deformation. This implies a horizontal structure at depth z_d that detaches the crustal displacement from the deeper lithosphere. The model runs show a qualitatively variable behaviour depending on the rates of displacement, in accord with the general notions discussed above. Provided that displacement rates are $<c.\,0.8\,\mathrm{mm\,a^{-1}}$ then conduction dominates the thermal evolution and cooling results from the ongoing deformation. At levels of 35–45 km this cooling amounts to *c.* 10–35°C for the displacement rates appropriate to the Alice Springs Orogen (as illustrated by the shaded zone in Fig. 14), which amounts to 33–50% of the long-term cooling predicted for the denudation.

Discussion

Our prime purpose in this contribution has been to illustrate the role played by tectonic processes in modifying heat source distributions in the crust in intraplate settings. The recognition that such modification must lead to long-term changes in the thermal structure of the crust, provided that the processes operate at sufficient horizontal length-scales, naturally leads to the notion that past tectonic history will modulate the response to subsequent tectonic processes or, more simply, to the notion of 'tectonic feedback'. Such tectonic feedback appears to have been particularly effective in modulating the response to intraplate deformation in central Australia during the Phanerozoic, in part because the central Australian crust was already strongly differentiated and, at least in comparison with typical continental crust, relatively enriched in heat producing elements. However, it is believed that such tectonic feedback should be an essential feature of the evolution of continental interiors. This is clearly evident when the thermal consequences of tectonic processes are formulated in terms of changes in h and q_c, and illustrated on the h–q_c plane (Fig. 15d, f). For example, typical crust might be expected to have q_c of $30\,\mathrm{mW\,m^{-2}}$, with a characteristic length scale of 7–10 km. Figure 8 shows that for such a crust, a 10% strain coupled with a surface process that in the long-term restores the original crustal thickness, will lead to long-term temperature changes of *c.* 20–30°C and that the repeated imposition of such strains over long

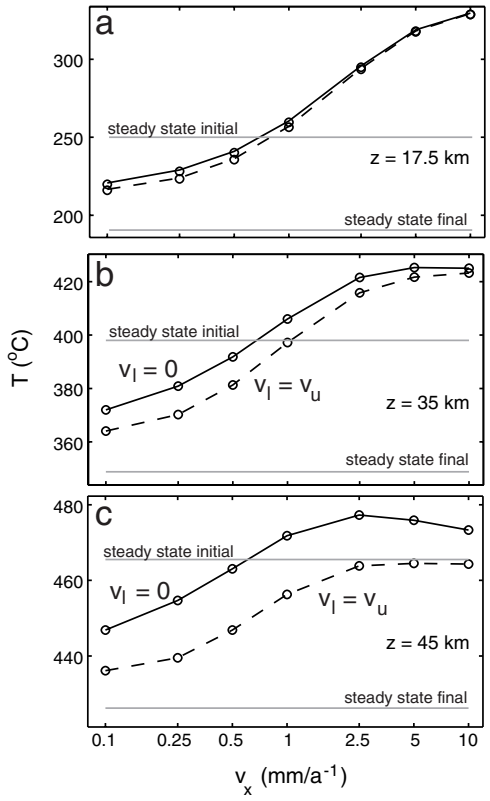

Fig. 14. Thermal consequences of displacement rate for kinematic model as shown in Figure 13. The temperatures shown correspond to positions above and below x_3 on Figure 13. The solid line shows the temperatures resulting after 15 km displacement (the inferred total Alice Springs displacement on the Redbank Shear Zone) at various rates of v_u with $v_l = 0$. The dashed line shows the equivalent temperatures with $v_l = v_u$. Steady state initial and final temperatures are indicated by the horizontal lines.

periods of geological time will lead to profound geochemical and thermal structuring of the crust (Fig. 15d, f). Even such subtle temperature changes are capable of producing dramatic changes in strength for a temperature-sensitive rheology, such as the 'Brace-Goetze' lithosphere (Fig. 9 & 10). Perhaps the most dramatic manifestation of this tectonic feedback is the extraordinary geophysical character of central Australia. Deformation during both the Petermann and Alice Springs Orogenies produced dramatic lateral variations in crustal density now manifest in the extraordinary gravity anomalies around the margins of the Amadeus Basin (Mathur 1976). The long-term preservation of these gravity anomalies implies significant lithospheric strength. The implication of a strong lithosphere is at odds with the localization of regional-scale intraplate deformation. The calculations summarized in Figure 13 indicate that lithospheric cooling (and by inference strengthening) will accompany intraplate deformation provided mean displacement rates are less than $c.0.5\,\mathrm{mm\,a^{-1}}$, and that erosion efficiently removes the topographic edifice. This potential for lithospheric-strengthening during ongoing deformation has important implications for the processes that lead to the cessation of deformation, and also to the way in which deformation shifts with time in the overall context of the orogen. If deformation were to cease as a result of ongoing lithospheric-strengthening, the lithosphere could potentially support a long-term isostatic imbalance by virtue of its acquired strength. Conceivably the preservation of the large gravity anomalies in central Australia reflects long-term strength increases arising as a consequence of the intraplate deformation. Furthermore, if slow rates of deformation lead to stripping of heat production over length-scales of $\geq$50 km, the distribution of relative lithospheric strength may change to the extent that deformation may shift to regions that have undergone less denudation. There is some evidence that regions in central Australia became 'stronger' as deformation and associated denudation proceeded. During the Alice Springs Orogeny, the major locus of deformation shifted away from the Redbank Shear Zone with time to similarly oriented structures 80–100 km into the interior of the orogen along the northern edge of the Ngalia Basin in the Early Carboniferous (Wells & Moss 1983). Conceivably this shift was controlled by an evolving thermal structure in the region around the Redbank Shear Zone that resulted in relative lithospheric strengthening despite the presence there of a crustal-scale discontinuity, favourably oriented to localize further deformation.

As a final discussion point, we consider the role that intraplate deformation, such as that observed in central Australia, plays in organizing the geochemical structure of the continental crust is considered. The chemical evolution of the continental crust is generally considered in terms of the primary crustal growth processes that arise from the depletion of the mantle in plate margin settings (e.g. O'Nions *et al.* 1979; McCulloch & Bennett 1994). While these models may account for the broad geochemical character of the continental crust, relatively little attention has been given to the subsequent geochemical structuring during post-crust forming processes. Geochemical structuring of the crust may occur in two main ways: (1) crustal differentiation

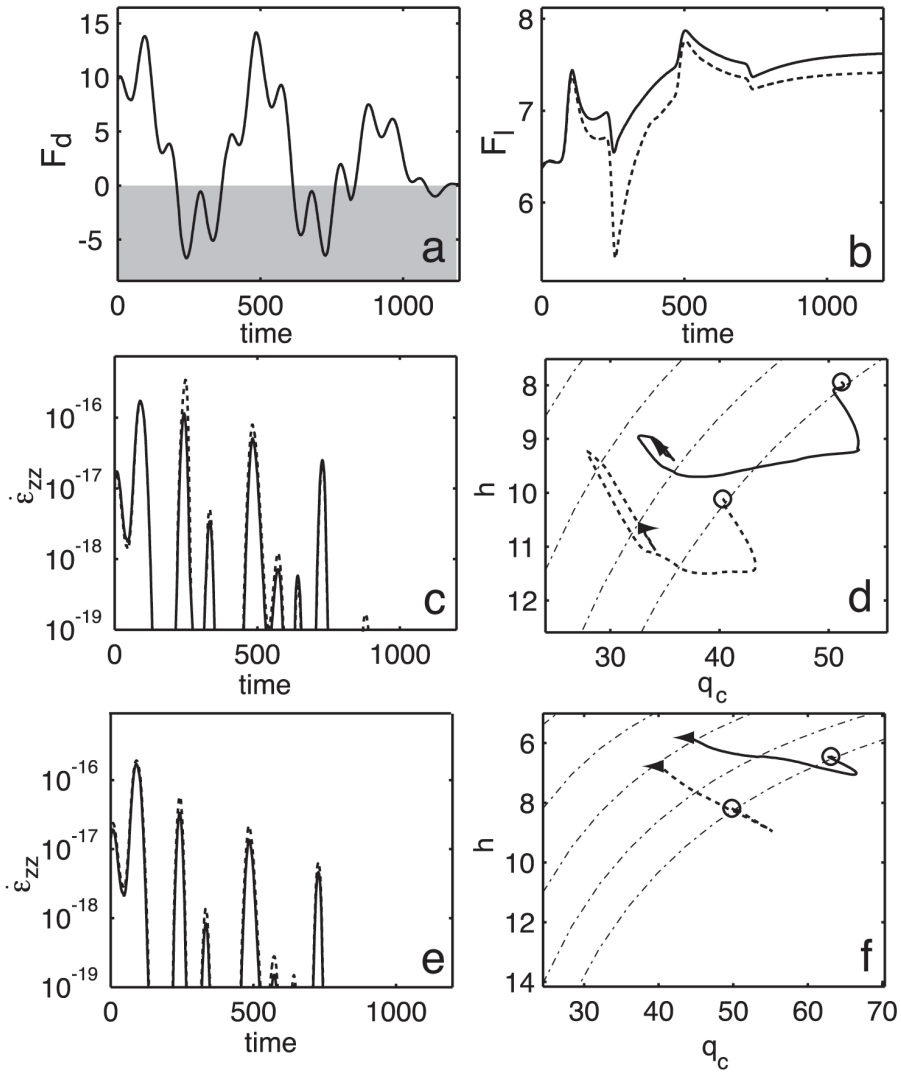

Fig. 15. The principle of "tectonic feedback" is illustrated with reference to numerical simulations in which a series of 1-D lithospheric columns (with temperature sensitive 'Brace-Goetze' rheology) are subject to a time-varying tectonic load (Fig. 15a, F_d in units of $10^{12}\,N\,m^{-1}$). Units of time are 10^6 years. The load oscillates on a time scale of several 100 Ma from compression ($F_d > 0$) to extension ($F_d < 0$). The response is expressed in terms of vertical stretching rate (ε_{zz} in units of s^{-1}, Figures 14c & 14e) and is determined by the interaction between the tectonic loading function and the evolving thermal and compositional structure of the column. The heat production parameters (expressed in terms of h and q_c, Figures 14d & 14f) evolve as a consequence of the deformation as well as surface processes (erosion and sedimentation) that act to restore the long-term surface elevation (initial and final h–q_c configurations are indicated by the circle and arrow heads, respectively). The strength of the lithosphere (F_l in units of $10^{12}\,N\,m^{-1}$, Fig. 15b) evolves as a function of its thermal and compositional structure, both due to transient and long-term changes. The figures show the evolution of a number of lithospheric columns that differ only in the way the heat sources are configured initially. Figure 15c & 14d show the results of simulations for two heat source distributions which initially approximate an inverse exponential dependence on depth, while Figure 15e & 14f show simulations for initial distributions in which heat production is confined to an upper crustal layer with thickness $\sim 2h$ of relatively uniform character. In all cases the heat production distributions are set so as to provide an identical Moho temperature so that initially the strength of the lithosphere is constant (Fig. 15b). In all simulations, the long-term effect of tectonic activity is to lower q_c (i.e. heat production is 'worked' out of the lithosphere) resulting in long-term increases in lithospheric strength. However, this is a strongly staged processes, with significant transient reductions in strength attendant with stretching events (i.e. at *c.* 250 and *c.* 750 Ma, Fig. 15b). Both Figure 15d & 14 illustrate a tendency for the long-term convergence of h–q_c parameters, suggesting that tectonic feedback provides may provide and effective agent for the long-term ordering of heat production in the continental crust.

associated with large-scale melt-transfer and (2) redistribution of material during deformation, sedimentation and erosion. The combination of these processes can dramatically affect the length scales associated with compositional variation in the crust. The formation of large mid-crustal granitic complexes of the type that characterize central Australia, effectively reduces the vertical length scale for the incompatible elements such as U, Th, K, Cs, Rb, Ba as well as SiO_2, by concentrating them at higher crustal levels. If these granites are subsequently exhumed, there is significant loss of the highly incompatible elements from the exhumed region. In an intraplate context, this material is deposited into intraplate basins, and may also be transported to continental margins in large drainage systems. This redistribution, which is a function of the tectonic history and hence thermal regime of the crust, fundamentally changes the chemical make up of the continental interior and, in so doing, its thermo-mechanical structure (Fig. 15). When compared to continental margins, there is very little likelihood of re-enriching a depleted continental interior via processes such as subduction. As such, intraplate deformation such as observed in central Australia, ultimately tends to drive existing heat production out of the crust (i.e., towards lower values of q_c – see Fig. 15). Indeed, such intraplate deformation may in fact be the prime reason that continental interiors have average heat production parameters of h *c.* 5–10 km and q_c *c.* 30–40 mW m^{-2}.

We thank Kerry Slater and the NTGS for supplying the airborne radiometric data used in the production of the heat production map of the Ormiston Gorge region, and Peter Haines for his contributions to our understanding of the duration of the Alice Springs Orogen. The organisers of the 'Orogenesis in the Outback' conference, particularly Jodie Miller, are thanked for their efforts in providing a wonderful and stimulating conference, during which the ideas discussed in this paper were presented. Ian Buick, Jean Braun and Bruce Goleby are thanked for their comments on the draft manuscript.

Appendix

This appendix outlines the reasoning that leads to the recognition that the length-scale in eqn. (4) is half the thickness of the heat producing layer, for the case where all crustal heat production is confined to an upper crustal layer of uniform heat production (Fig. 6a). For such a distribution, the temperature field in the layer is given by:

$$T_z = -\frac{q_r z}{k} + \frac{H_s z(h_r - z/2)}{k} \qquad \text{(A1)}$$

where H_s, is the heat production in the heat producing layer; h_r, is the thickness of the heat producing layer; and k, is the thermal conductivity. In eqn. (A1) the first term on the right represents the component of the temperature field due to the heat flow from beneath the heat producing parts of the lithosphere (dashed line in Fig. 6b). The second term on the right represents the contribution due to heat sources in the crust (Fig. 6c). This is used to define the quantity, T_{q_c}, the temperature contribution at any due to heat production in the crust. Figure 6c shows that T_{q_c} reaches its maximum value (T'_{q_c}) at the base of the heat-producing layer. The appropriate expressions for T'_{q_c} for this model is therefore:

$$T'_{q_c} = \frac{H_s h_r^2}{2k} \qquad \text{(A2)}$$

Equating eqn. (A2) with equation (3) and noting that q_c equals $H_s h_r$, yields $h = h_r/2$.

References

BEAUMONT, C., FULLSACK, P. & HAMILTON, J. 1994. Styles of crustal deformation caused by subduction of the underlying lithosphere. *Tectonophysics*, **232**, 119–132.

BRACE, W. F. & KOHLSTEDT, D. L. 1980. Limits on lithospheric strength imposed by laboratory experiments. *Journal of Geophysical Research*, **85**, 6248–6252.

BRADSHAW, J. D. & EVANS, P. R. 1988. Paleozoic tectonics, Amadeus Basin, central Australia. *In*: MOORE, D. B. (ed.) *Technical papers 1988 APEA conference*. Australian Petroleum Exploration Association, **28**, 267–282.

BRAUN, J. 1992. Postextensional mantle healing and episodic extension in the Canning Basin. *Journal of Geophysical Research*, **97**, 8977–8936.

BRAUN, J. & SHAW, R. D. 1998. Contrasting styles of lithospheric deformation along the northern margin of the Amadeus Basin, central Australia. *In*: BRAUN, J., DOOLEY, B., GOLEBY, B. R., VAN DER HILST, R. D. & KLOOTWIJK, C. (eds) *Structure and Evolution of the Australian Continent*. American Geophysical Union Geodynamic Series, **26**.

CAMACHO, A., VERNON, R. H. & FITZGERALD, J. D. 1995. Large volumes of anhydrous pseudotachylite in the Woodroffe Thrust, eastern Musgrave Ranges, Australia. *Journal of Structural Geology*, **17**, 371–383.

CAMACHO, A., COMPSTON, W., MCCULLOCH, M. & MCDOUGALL, I. 1997. Timing and exhumation of eclogite facies shear zones, Musgrave Inlier, Central Australia. *Journal of Metamorphic Geology,* **15**, 735–751.

CULL, J. P. 1982. An appraisal of Australian heat-flow data. *BMR Journal of Geology and Geophysics*, **7**, 11–21.

DUNLAP, W. J. & TEYSSIER, C. 1995. Palaeozoic deformation and isotopic disturbance in the south-eastern Arunta Inlier, Australia. *Precambrian Research*, **71**, 229–250 1995.

DUNLAP, W. J., TEYSSIER, C., MCDOUGALL, I. & BALDWIN, S. 1995. Thermal and structural evolution of the intracratonic Arltunga nappe complex, central Australia. *Tectonics*, **14**, 1182–1204

EDGOOSE, C. J., CAMACHO, A., WAKELIN-KING, G. A. & SIMONS, B. A. 1993. Kulgera, Northern Territory. 1:250 000 Geological sheet and explanatory notes. Northern Territory Geological Survey, Darwin, Australia.

FLÖTTMANN, T. & HAND, M. 1999. Folded basement-cored tectonic wedges along the northern Amadeus Basin, Central Australia: constraints on intracontinental orogenic shortening. *Journal of Structural Geology*, **21**, 399–412.

FORMAN, D. J. 1971. The Arltunga Nappe Complex, MacDonnell Ranges, Northern Territory, Australia. *Journal of the Geological Society of Australia*, **18**, 173–182.

GOLEBY, B. R., WRIGHT, C., COLLINS, C. D. N. & KENNETT, B. L. N. 1988. Seismic reflection and refraction profiling across the Arunta Inlier and the Ngalia and Amadeus Basins. *Australian Journal of Earth Sciences*, **35**, 275–294.

GOLEBY, B. R., SHAW, R. D., WRIGHT, C., KENNETT, B. L. N. & LAMBECK, K. 1989. Geophysical evidence for 'thick-skinned' crustal deformation in central Australia. *Nature*, **337**(6205), 325–330.

HAND, M. & SANDIFORD, M. 1999. Intraplate deformation in central Australia, the link between subsidence and fault reactivation. *Tectonophysics*, **305**, 121–140.

HAINES., P. W., BAGAS, L., WYCHE, S., SIMONS, B. & MORRIS, D. G. 1991. *Barrow Creek*. 1:250 000 Geological sheet and explanatory notes. Northern Territory Geological Survey, Darwin, Australia.

HOSKINS, D. & LEMON, N. 1995. Tectonic development of the eastern Officer Basin. *Exploration Geophysics*, **26**, 395–402.

JONES, B. G. 1972. Upper Devonian to lower Carboniferous stratigraphy of the Pertnjara Group, Amadeus Basin, central Australia. *Journal of the Geological Society of Australia*, **19**, 229–249.

JONES, B. G. 1991. Fluvial and lacustrine facies in the Middle to Late Devonian Pertnjara Group, Amadeus Basin, Northern Territory, and their relationship to tectonic events and climate. *In*: KORSCH, R. J. & KENNARD, J. M. (eds) *Geological and geophysical studies of the Amadeus Basin, central Australia*. Bulletin of the Bureau of Mineral Resources, **236**, 333–348.

KORSCH, R. J., GOLEBY, B. R., LEVEN, J. H. & DRUMMOND, B. J. 1998. Crustal architecture of central Australia based on deep seismic reflection profiling. *Tectonophysics*, **288**, 57–69.

LAMBECK, K. & BURGESS, G. 1992. Deep crustal structure of the Musgrave Inlier, central Australia: results from teleseismic travel-time anomalies. *Australian Journal of Earth Sciences*, **39**, 1–19.

LINDSAY, J. F. & LEVEN, J. H. 1996. Evolution of a Neoproterozoic to Palaeozoic intracratonic setting, Officer Basin, South Australia. *Basin Research*, **8**, 403–424.

MABOKO, M. A. H., MCDOUGALL, I., ZEITLER, P. K. & WILLIAMS, I. S. 1992. Geochronological evidence for *c.* 530–550 Ma juxtaposition of two Proterozoic metamorphic terrains in the Musgrave Ranges, central Australia. *Australian Journal of Earth Sciences*, **39**, 457–471.

MATHUR, S. P. 1976. Relation of Bouguer anomalies to crustal structure in southwestern and central Australia. *BMR Journal of Australian Geology and Geophysics*, **1**, 277–286.

MAWBY, J., HAND., M. & FODEN, J. 1999. Sm–Nd evidence for high-grade Ordovician metamorphism in the Arunta Inlier, central Australia. *Journal of Metamorphic Geology*, **17**, 653–668.

MCLENNAN, S. M. & TAYLOR, S. R. 1996. Heat flow and chemical composition of continental crust. *Journal of Geology*, **104**, 369–377.

MCCULLOCH, M. T. & BENNETT, V. C. 1994. Progressive growth of the earth's continental crust and depleted mantle: geochemical constraints. *Geochimica et Cosmochimica Acta*, **58**, 4717–4738.

OFFE, L. A. 1978. *Mount Peake, Northern Territory*. 1:1:250 000 geological map series. Australian Bureau of Mineral Resources, Australia.

O'NIONS, R. K., EVENSEN, N. M. & HAMILTON, P. J. 1979. Geochemical modeling of mantle differentiation and crustal growth. *Journal of Geophysical Research*, **84**, 6091–6101.

PATERSON, M. S. 1987. Problems in the extrapolation of laboratory rheological data. *Tectonophysics*, **133**, 33–43.

SANDIFORD, M. 1999. Mechanics of basin inversion. *Tectonophysics*, **305**, 109–120.

SANDIFORD, M. & HAND, M. 1998*a*. Controls on the locus of Phanerozoic intraplate deformation in central Australia. *Earth and Planetary Science Letters*, **162**, 97–110.

SANDIFORD, M. & HAND, M. 1998*b*. Australian Proterozoic high-temperature metamorphism in the conductive limit. *In*: TRELOAR, P. & O'BRIEN, P. (eds) *What Controls Metamorphism*. Geological Society, London, Special Publications, **138**, 103–114.

SANDIFORD, M., PAUL, E. & FLÖTTMANN, T. 1988. Sedimentary thickness variations and deformation intensity during basin inversion in the Flinders Rangers, South Austrralia. *Journal of Structural Geology*, **30**, 1721–1731.

SCRIMGEOUR, I. & CLOSE, D. 1998. Regional high pressure metamorphism during intracratonic deformation: the Petermann Orogeny, central Australia. *Journal of Metamorphic Geology*, **17**, 557–572

SHAW, R. D. & BLACK, L. P. 1991. The history and tectonic implications of the Redbank Thrust Zone, central Australia, based on structural, metamorphic and Rb–Sr isotopic evidence. *Australian Journal of Earth Science,* **38**, 307–332.

SHAW, R. D., ETHERIDGE, M. A. & LAMBECK, K. 1991*a*. Development of the late Proterozoic to mid-Palaeozoic intracratonic Amadeus Basin in central Australia: A key to understanding tectonic forces in plate interiors. *Tectonics*, **10**, 688–721.

SHAW, R. D., KORSCH, R. J., WRIGHT, C. & GOLEBY, B. R. 1991*b*. Seismic interpretation and thrust tectonics of the Amadeus Basin, central Australia, along the BMR regional seismic line. *In*: KORSCH,

R. J. & KENNARD, J. M. (eds) Ge*ological and geophysical studies in the Amadeus Basin, central Australia*. Australian Bureau Mineral Resources Bulletin, **236**, 385–408.

SONDER, L. & ENGLAND, P. C. 1986. Vertical averages of rheology of the continental lithosphere; relation to thin sheet parameters. *Earth and Planetary Science Letters*, **77**, 81–90.

STEWART, A. J. 1995. Western extension of the Woodroffe Thrust, Musgrave Inlier, central Australia. *AGSO Journal of Geology and Geophysics*, **16**, 147–153.

TEYSSIER, C. 1985. A crustal thrust system in an intracratonic environment. *Journal of Structural Geology*, **7**, 689–700.

VAN DER HILST, R. D., KENNETT, B. L. N. & SHIBUTANI, T. 1998. Upper mantle structure beneath Australia from portable array deployments. *In*: BRAUN, J., DOOLEY, R., GOLEBY, B., VAN DER HILST, R. D. & KLOOTWIJK, C. (eds) *Structure and Evolution of the Australian Continent*. American Geophysical Union Geodynamic Series, **26**, 39–58.

WALTER, M. R. & GORTER, J. D. 1994. The Neoproterozoic Centralian Superbasin in Western Australia: the Savory and Officer Basins. *In*: PURCELL, P. G. & PURCELL, R. R. (eds) *The sedimentary basins of Western Australia*. Proceedings Petroleum Exploration Society Australia Symposium, Perth, 851–864.

WALTER, M. R., VEEVERS, J. J., CALVER, C. R. & GREY, K. 1995. Neoproterozoic stratigraphy of the Centralian Superbasin, Australia. *Precambrian Research*, **73**, 173–195.

WARREN, R. G. & HENSEN, B. J. 1989. The P–T evolution of the Proterozoic Arunta Inlier, central Australia, and implications for tectonic evolution. *In*: DALY, J. S., CLIFF, R. A. & YARDLEY, B. W. D. (eds) *Evolution of metamorphic belts*. Geological Society, London, Special Publications, **43**, 349–355.

WELLS, A. T. 1982. *Napperby, Northern Territory*. 1:1:250 000 geological map series. Australian Bureau of Mineral Resources (Canberra), Australia.

WELLS, A. T. & MOSS, F. J. 1983. The Ngalia Basin, Northern Territory; stratigraphy and structure. *Australian Bureau Mineral Resources Geology and Geophysics Bulletin*, **212**, 88.

WELLS, A. T., FORMAN, D. J., RANFORD, L. C. & COOK, P. J. 1970. Geology of the Amadeus Basin, central Australia. *Australian Bureau Mineral Research Geology and Geophysics Bulletin*, **100**.

YOUNG, D. N., FANNING, C. M., SHAW, R. D., EDGOOSE, C. J., BLAKE, D. H., PAGE, R. W. & CAMACHO, A. 1995. U–Pb zircon dating of tectonomagmatic events in the northern Arunta Inlier, central Australia. *Precambrian Research*, **71**, 45–68.

ZIELHUIS, A. & VAN DER HILST, R. D. 1996. Upper-mantle shear velocity beneath eastern Australia from inversion of waveforms from Skippy portable arrays. *Geophysical Journal International*, **127**, 1–16.